



Impact of irrigation on South Asian monsoon climate

Fahad Saeed



Hinweis

Die Berichte zur Erdsystemforschung werden vom Max-Planck-Institut für Meteorologie in Hamburg in unregelmäßiger Abfolge herausgegeben.

Sie enthalten wissenschaftliche und technische Beiträge, inklusive Dissertationen.

Die Beiträge geben nicht notwendigerweise die Auffassung des Instituts wieder.

Die "Berichte zur Erdsystemforschung" führen die vorherigen Reihen "Reports" und "Examensarbeiten" weiter.



Notice

The Reports on Earth System Science are published by the Max Planck Institute for Meteorology in Hamburg. They appear in irregular intervals.

They contain scientific and technical contributions, including Ph. D. theses.

The Reports do not necessarily reflect the opinion of the Institute.

The "Reports on Earth System Science" continue the former "Reports" and "Examensarbeiten" of the Max Planck Institute.

Anschrift / Address

Max-Planck-Institut für Meteorologie
Bundesstrasse 53
20146 Hamburg
Deutschland

Tel.: +49-(0)40-4 11 73-0
Fax: +49-(0)40-4 11 73-298
Web: www.mpimet.mpg.de

Layout:

Bettina Diallo, PR & Grafik

Titelfotos:

vorne:

Christian Klepp - Jochem Marotzke - Christian Klepp

hinten:

Clotilde Dubois - Christian Klepp - Katsumasa Tanaka

Impact of irrigation on South Asian monsoon climate

Fahad Saeed

aus Wah Cantt, Pakistan

Hamburg 2011

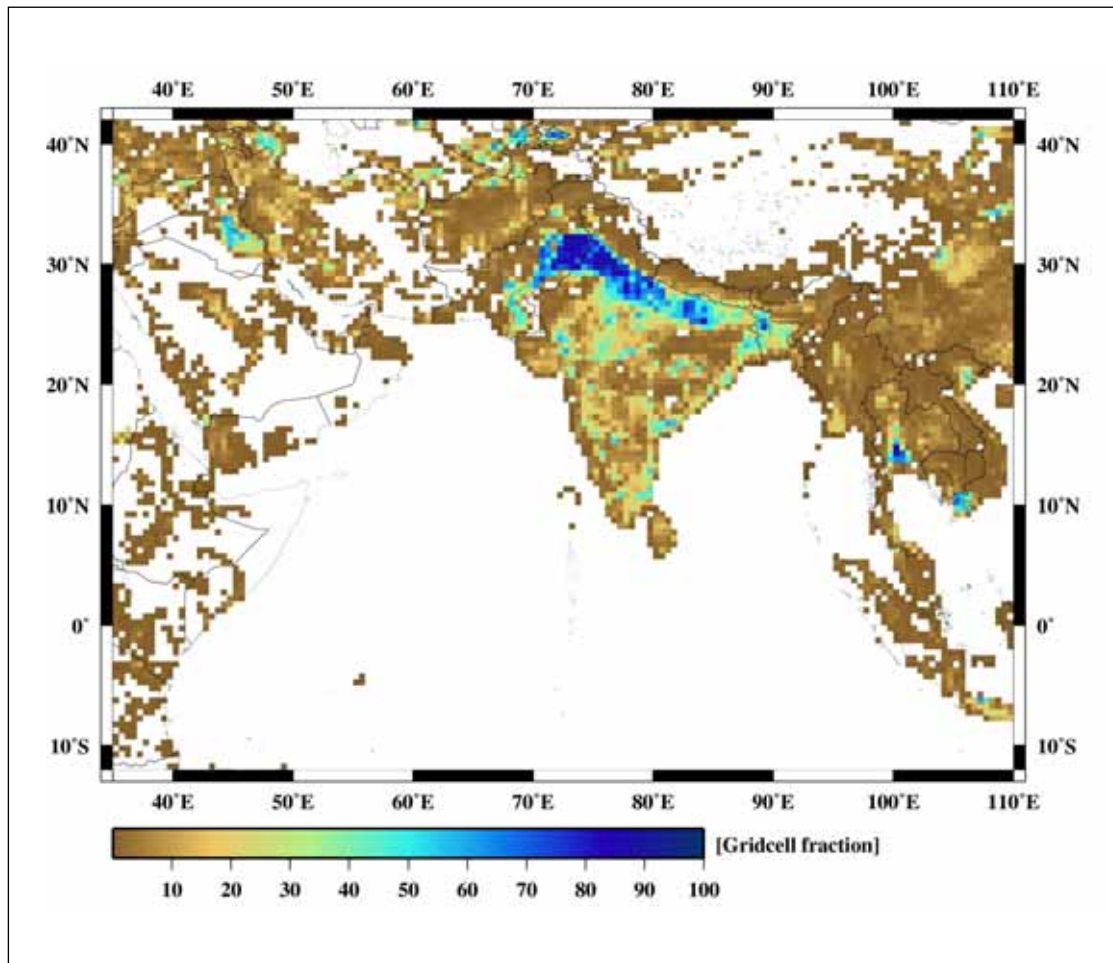
Fahad Saeed
Max-Planck-Institut für Meteorologie
Bundesstrasse 53
20146 Hamburg
Germany

Als Dissertation angenommen
vom Department Geowissenschaften der Universität Hamburg

auf Grund der Gutachten von
Prof. Dr. Martin Claussen
und
Dr. Stefan Hagemann

Hamburg, den 13. Juli 2011
Prof. Dr. Jürgen Oßenbrügge
Leiter des Departments für Geowissenschaften

Impact of irrigation on South Asian monsoon climate



Fahad Saeed

Hamburg 2011

Contents

1	Introduction	7
2	Impact of irrigation on South Asian summer monsoon	11
2.1	Introduction	11
2.2	Methods	12
2.3	REMO-Baseline	13
2.4	REMO-Irrigation	15
2.5	Conclusions	20
3	A framework for the evaluation of SASM applied to REMO	21
3.1	Introduction	21
3.2	Model and experimental setup	22
3.3	Evaluation framework	23
3.4	Results	26
3.4.1	Winds	26
3.4.2	Correlation between precipitation and circulation indices	28
3.4.3	ITCZ indices	31
3.4.4	Onset indices	31
3.4.5	MTG and ESZW indices	31
3.5	Summary and conclusion	32
4	Influence of mid-latitude circulation on UIB precipitation: the role of irrigation	35
4.1	Introduction	35
4.2	Data and methodology	37
4.3	Mid-latitudinal influence on the precipitation over UIB	38
4.3.1	Proposed mechanisms influencing precipitation over UIB	41
4.4	Irrigation Experiment	44
4.4.1	Simplified irrigation scheme	45
4.4.2	Model validation and impact of irrigation	48
4.5	Summary and Discussion	53
5	Conclusions and Outlook	57
5.1	Summary	57
5.2	Outlook	59
6	Acknowledgements	61

Abstract

The land surface and atmosphere have multiple pathways to interact with each other, which include the coupled water and energy cycle. This coupling plays an imperative role in the monsoon climate of South Asia which is manifested as a strongly coupled land-atmosphere-ocean circulation system. Different feedbacks occur when land and atmosphere interact and the understanding of these feedbacks is very crucial to explain past climatic changes and to improve the knowledge of seasonal weather forecasts and future climate. Considering the strongly coupled nature of the South Asian summer monsoon (SASM), the soil moisture conditions become very crucial both for interannual as well as intraseasonal precipitation. For South Asia, the water used for irrigation plays a major role in modifying soil moisture conditions, which in turn effects the monsoon circulation and precipitation.

The Indian subcontinent is one of the most intensely irrigated regions of the world and state of the art climate models do not account for the representation of irrigation. Sensitivity studies with the regional climate model REMO show distinct feedbacks between the simulation of the monsoon circulation with and without irrigation processes. It is found that the temperature and mean sea level pressure, where the standard REMO version without irrigation shows a significant bias over the Indus and Ganges basins, are highly sensitive to the water used for irrigation. In the sensitivity test with the representation of irrigation in REMO, the removal of this bias is achieved, which resulted in less differential heating between land and sea masses. This in turn reduces the westerlies entering into the land from the Arabian Sea, hence creating conditions favorable for currents from the Bay of Bengal to intrude deep into western India and Pakistan that have been unrealistically suppressed before. Therefore, it is concluded that the representation of irrigated water is unavoidable for the realistic simulation of South Asian summer monsoon and its response under global warming.

Further, considering the complex spatial and deep vertical structure of SASM, the existing literature on the validation of a climate model dealing with only a few surface variables over the region is considered insufficient. Therefore, an evaluation framework has been proposed for the better assessment of the capability of a climate model in capturing the fundamental structure of SASM. This framework has been applied to the regional climate model REMO using ERA40 lateral boundary conditions for the period 1961–2000. The application of the framework yielded satisfactory performance of REMO in capturing the lower, middle, and upper components of the SASM circulation. REMO has higher correlation between different SASM indices as compared to ERA40, showing its ability in capturing the dynamical link between these indices better than ERA40.

We have employed different criteria for the assessment of the monsoon onset, and the movement of the Intertropical Convergence Zone (ITCZ) during the boreal summer and REMO has captured these phenomena reasonably well. The model has also shown the association of the meridional temperature gradient with the easterly shear of zonal winds. These results lead to the conclusion that REMO is well suited for long-term climate change simulations to examine projected future changes in the complex SASM system.

Afterwards, the attention is given to the Indus river which has the largest contiguous irrigation system in the world. Since much of the flow of the Indus river originates in the Himalayan, Karakoram and Hindu Kush mountains, an understanding of weather characteristics leading to precipitation over the region is essential for water resources management. The study examines the influence of upper level mid-latitude circulation on the summer precipitation over the upper Indus basin (UIB). Using reanalysis data, a geopotential height index (GH) is defined at 200 hPa over central Asia, which has a significant correlation with the precipitation over UIB. GH has also shown significant correlation with the heat low (over Iran and Afghanistan and adjoining Pakistan), easterly shear of zonal winds (associated with central Asian high) and evapotranspiration (over UIB). It is argued that the geopotential height index has the potential to serve as a precursor for the precipitation over UIB. In order to assess the influence of irrigation on precipitation over UIB, a simplified irrigation scheme has been developed and applied to the regional climate model REMO. It has been shown that both versions of REMO (with and without irrigation) show significant correlations of GH with easterly wind shear and heat low. However, contrary to reanalysis and the REMO version with irrigation, the REMO version without irrigation does not show any correlation between GH index and evapotranspiration as well as between geopotential height and precipitation over UIB.

It is concluded that although atmospheric moisture over the coastal Arabian sea region, triggered by wind shear and advected northward due to the heat low, also contribute to the UIB precipitation. However for the availability of necessary moisture for precipitation over UIB, the major role is played by the evapotranspiration of water from irrigation. From the results, it may also be inferred that the representation of irrigated water in climate models is unavoidable for the representation of SASM climate.

1 Introduction

The South Asia region is a home to one-sixth of the world's population making it the most densely populated region of the world. About 70% of South Asia's population lives in rural areas, and most of the rural population depends on agriculture for its livelihood. Agriculture employs about 60% of the labour force in South Asia and contributes 22% of regional Gross Domestic Product (GDP; World-Bank (2008)). Therefore agriculture is, and will likely remain an important sector of the economy in terms of food production as well as employment generation. Agriculture, for its irrigated as well as rainfed crops, depends heavily on the seasonal precipitation. Therefore, understanding of the processes leading to the seasonal precipitation is of utmost importance for the agrarian economy of the region.

Water availability in South Asia is driven by monsoons and western disturbances. Two monsoon systems operate in the region: The southwest or summer monsoon and the northeast or winter monsoon. The summer monsoon accounts for 70%-90% of the annual rainfall over most of South Asia, except over Sri Lanka and Maldives where the northeast monsoon is dominant in the winter. Apart from monsoons, the northwestern part of South Asia comprising of northern Pakistan and northwestern India, also receives considerable precipitation in the form of snow from western disturbances which originate from the Mediterranean sea in winter.

The South Asian region contains a number of large rivers of which Ganges, Brahmaputra, Meghna, Indus, Godavari, Mahanadi and Narmada are the prominent ones. The main contributor to Ganges, Brahmaputra and Indus (also called as Himalayan rivers) is the melt water from snow (and glaciers) which is accumulated in the winter season in the northwestern part of South Asia. Due to precipitation both in winter (western disturbances) and summer monsoon, the Himalayan rivers remain perennial throughout the year. However, excessive melt along with the arrival of monsoon cause a prominent peak in the annual discharge curve for these rivers. Apart from the Himalayan rivers, the rest of the rivers are mainly rainfed. According to an estimate, the snow and rainfed river basins occupy 2.32 million km² or 55% of basin areas while the remaining 1.90 million km² or 45% of basin areas belong to rainfed rivers (Mirza and Ahmed, 2005).

In the densely populated region of South Asia, life has always been vulnerable to extremes and shifts in climate, but in the last couple of decades evidence is growing that human activities have now reached a level where they make the weather pattern and climate stability more vulnerable (Cotton and Pielke, 2007). Although much of the research in this regard is focused on the direct effects of human activities on atmospheric composition, it is also documented that human induced landscape changes can affect atmospheric processes from local to regional weather patterns (Cotton and Pielke, 2007). In the monsoon climate such as South Asia, where the land atmosphere interaction

1 Introduction

plays a vital role in the development and evolution of monsoon, such human induced changes become very crucial. For many regions around the world, the rapid increase of irrigated land during the last century has significantly affected the hydrological cycle and energy budget at the land surface. This has motivated researchers to look into the potential impacts of the irrigation on regional and global climate (Boucher et al., 2004; Lobell et al., 2006). These studies support the concept, that depending upon the spatial extent of irrigation and the degree to which a region's atmosphere is linked to its land surface processes, the current irrigation significantly alters the climate in some areas. One of the most important direct impacts of irrigation on the climate is the reduction of near surface temperature through changes from sensible to latent heat fluxes (Kueppers et al., 2007). The enhanced availability of moisture due to irrigation may lead to increased evapotranspiration, resulting in more cloud cover due to convection and hence precipitation (Pielke, 2001), which is also known as local recycling of moisture. Irrigation effects on climate can also be indirect especially in the monsoon regions where the advection of moisture is governed by the land sea thermal contrast. Based on this linkage it can be hypothesized that the magnitude of temperature reduction in certain regions due to irrigation may be comparable to or even exceed the effects of other climate forcings. The biggest implication of this can be that the global warming signal has been "masked" in certain regions by irrigation-related cooling (Kueppers et al., 2007).

South Asia is the most densely irrigated region in the world. In order to cope with the threatening expansion of population, rapid expansion of irrigated land took place and according to an estimate the irrigated area in South Asia doubled over the last four decades of the 20th century (Barker and Molle, 2004). Therefore irrigation is believed to influence the climate of South Asia very strongly via land atmosphere interaction. However, there have not been many studies contributing to our understanding of potential impact of irrigation on South Asian climate. Furthermore, it is extremely difficult to quantify the role of feedbacks from irrigation with the help of using the observed data only. Therefore, the potential effect of irrigation in affecting the climate of the region is usually discussed based upon climate model experiments.

Within this thesis the strengths and weaknesses of the regional climate model REMO to simulate the region's climate characteristics are assessed. In addition, a representation of irrigation is introduced in the REMO model in order to investigate the changes caused by irrigation to the atmospheric processes over South Asia. Based on the existing lack of research regarding the footprint of irrigation on the climate of South Asia, several research questions emerge. These questions are:

- i.) Considering the complex spatial and deep vertical structure, does REMO have the ability to adequately simulate the climate associated with SASM? What could be the criteria for evaluating the performance of a climate model over South Asian region?
- ii.) What are the prominent biases shown by REMO over the SASM region and what are the causes leading to these biases?
- iii.) How crucial is the representation of irrigation in a climate model for its application over the South Asian region and does REMO show better performance of the SASM with the representation of irrigation?
- iv.) Is there any linkage between the mid-latitude circulation and rainfall over the

upper Indus basin? If such a link exists, what is the role of irrigation in describing it?

The objective of this thesis is to contribute to answer the above mentioned research questions. For this purpose, a number of simulations have been conducted and analysed using the REMO model at different time scales. These simulations include the execution of REMO in its baseline mode, with the simple representation of irrigation and with the implementation of a more sophisticated irrigation scheme. All these simulations are validated against different observed as well as reanalysis datasets.

Each of the chapters from 2 to 4 is designed to be an independent and full paper, thus some repetitions may inevitably occur in data and method descriptions. Note that the references from all chapters will be gathered together into a reference list at the end of the thesis.

Chapter 2 deals with the application of REMO over the South Asian region. A sensitivity experiment with irrigation is presented and the impact of irrigation on SASM circulation is discussed. This chapter has been published in a peer reviewed journal (Saeed et al., 2009a).

In chapter 3, a framework for the evaluation of a regional climate model over SASM region is proposed. This framework is applied to REMO in order to assess the ability of the model in capturing the deep vertical structure associated with SASM. This chapter has also been published in a peer reviewed journal (Saeed et al., 2011a).

Chapter 4 of this thesis is focused on the influence of mid-latitude circulation on precipitation over the Indus basin. In order to assess the role of irrigation in bridging the two of them, a simplified irrigation scheme is developed and applied to REMO. This chapter has been submitted for a peer reviewed publication (Saeed et al., 2011b).

Chapter 5 summarizes the findings of the thesis with respect to the above mentioned research questions. Moreover an outlook for future work in terms of climate change studies over the South Asian region is presented.

2 Impact of irrigation on South Asian summer monsoon

2.1 Introduction

With dependence of 22% of world's population on its annual rainfall, South Asian Summer Monsoon (SASM) plays a crucial role by effecting water resources, agriculture, economics and human mortality of the region. Given the reliance of lives and economies of many countries in Asia on monsoon rainfall (Cadet, 1979), the understanding of processes affecting the monsoon is an issue of both scientific and societal importance.

Since South Asia is one of the most intensely irrigated regions of the world (Sacks et al., 2009), the role of irrigation in modifying the local climate through feed back mechanisms has been well recognized in earlier studies. de Rosnay et al. (2003) conducted a two year model simulation directed by the 1987–1988 International Satellite Land Surface Climatology Project data sets by coupling an irrigation module with a land surface model and compared the effects of irrigated against non-irrigated land over the subcontinent. Douglas et al. (2006) presented a conceptual approach and investigated the changes across India between a pre-agriculture and a contemporary agriculture land cover. Both of these studies deal with the irrigation effect on the atmospheric moisture and energy vertical fluxes, but do not take into account the effects on large-scale SASM circulations. More recently, Lee et al. (2009) highlighted the importance of irrigation over the India by statistically associating the changes of observed rainfall with irrigation. Douglas et al. (2009) simulated a five-day monsoon event using different crop scenarios and identified changes in circulation patterns and precipitation over India. Considering the complexity of processes and influence of different regions involved in the SASM phenomenon, there is a need of evaluation of irrigation affects over larger domain and longer time scale.

Since more than a decade, the heat low over Pakistan and adjoining north-west India is used as an important predictor for SASM rainfall (Singh et al., 1995). The major part of this heat low region falls inside the densely irrigated Indus basin, which has been used for irrigation since ancient times (Figure 2.1).

The Indus basin is the largest contiguous irrigation network in the world and its surface water is heavily manipulated by building large dams, link canals, watercourses etc. and hence resulting in modification of the amount of water in soil (Khan et al., 2008). It is estimated that the Indus River drains only one-eighth of the $\sim 400 \text{ km}^3$ water that annually falls on the basin in the form of rain and snow, with the remainder

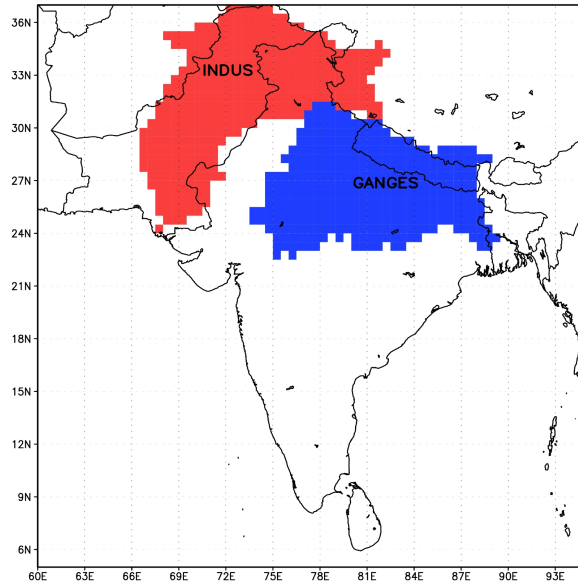


Figure 2.1: Location of Indus and Ganges basin at 0.5° resolution in South Asia region.

used mostly for irrigation and returned to the atmosphere by evapotranspiration (ET) (Karim and Veizer, 2002). Therefore, it can be assumed that this huge manipulation of water for irrigation would modulate the local climate occurring in the heat low region and therefore may effect the large-scale SASM's circulations.

2.2 Methods

In this study Max Planck Institute's REgional MOdel (REMO) has been applied over South Asian domain (Jacob, 2001; Jacob et al., 2007), forced with so called "perfect" lateral boundary conditions obtained from the European Centre for Medium Range Weather Forecasts reanalysis (ERA40) (Uppala et al., 2005). REMO has been applied at a resolution of 0.5 degree (~ 55 km) over the South Asian domain which encompasses 12°S to 42°N and 35°E to 110°E with 109 grid points along the latitude and 151 grid points along the longitudinal direction. All the results presented are averaged over four monsoon months June, July, August and September.

The first simulation comprises of 40 years from 1961 to 2000 (REMO-baseline), three years from 1958 to 1960 are considered as spin up. In the second simulation, in order to take into account the effect of irrigation, we conducted a sensitivity simulation using a map of irrigated areas as shown in Figure 2.2 (Siebert et al., 2005). This is then remapped to 0.5-degree resolution and brought to the REMO South Asian model domain. For the irrigated fraction of a grid box, we have increased the soil wetness to a critical value in each time step, so that potential ET can occur. In REMO, following Roeckner et al. (1996), this value is set to 75% of the soil water holding capacity by assuming that

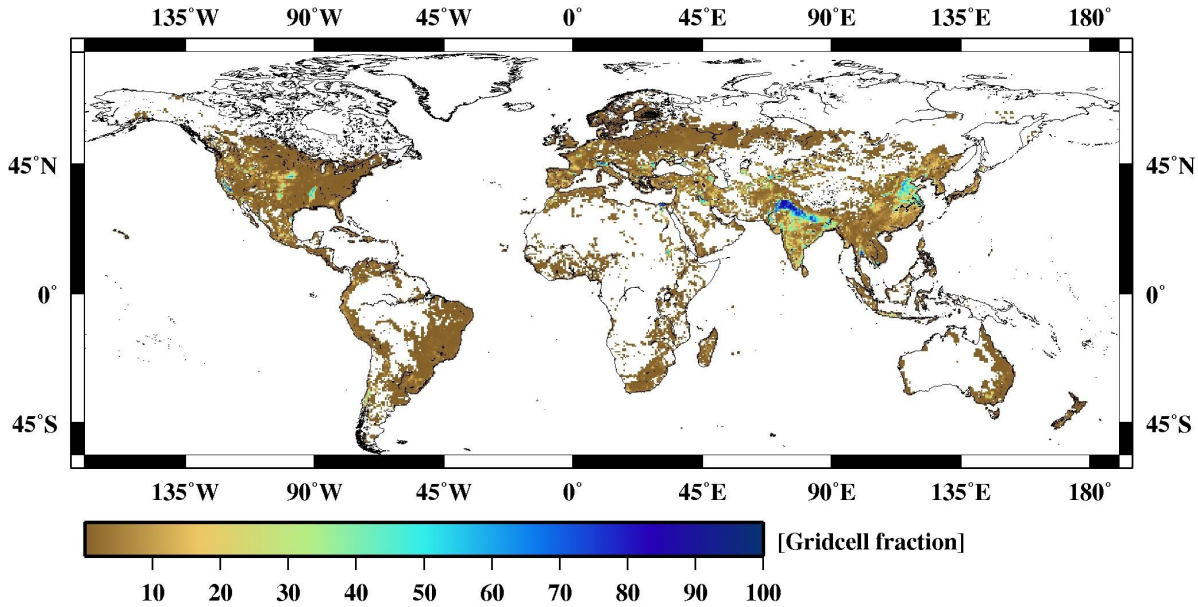


Figure 2.2: Irrigation map of the world showing fraction of irrigated area to total area of grid box.

irrigation is conducted to fulfill optimal conditions for the vegetation/crops, so that they can transpire at a potential rate. The sensitivity experiment is conducted from 1986–1992 with the initial three years discarded as spin up for new soil moisture conditions (REMO-irrigation).

2.3 REMO-Baseline

Considering “notoriously difficult to predict” nature of SASM (Jayaraman, 2005), model has reproduced a number of important features satisfactorily in REMO-baseline experiment. It has simulated the characteristic wide range of 2m temperatures, ranging from more than 40°C in Pakistan, to less than 0°C over the Himalayas (Figures 2.3(a) and (b)). Over the Indian subcontinent, the model is characterized by a warm temperature bias of up to several degrees for most of the land areas. The largest deviation exceeding 5°C occurs over the heat low regions of the Indus basin as discussed above. The model simulates the location of heat low region, however the overestimation of temperature has caused an acute underestimation of sea level pressure (MSLP) (Figures 2.3(c) and (d)). This has resulted into increased differential heating between ocean and land, and therefore the overestimation of winds entering into the plains of the Indian subcontinent from the Arabian Sea (Figures 2.3(e) and (f)). In monsoon break periods, these winds play a passive role when monsoon currents from Bay of Bengal (BOB) are shifted towards northern India along the foothills of Himalaya and towards southern peninsula, allowing more westerlies to intrude inside the plains of central India (Prasad et al., 2007). In our

2 Impact of irrigation on South Asian summer monsoon

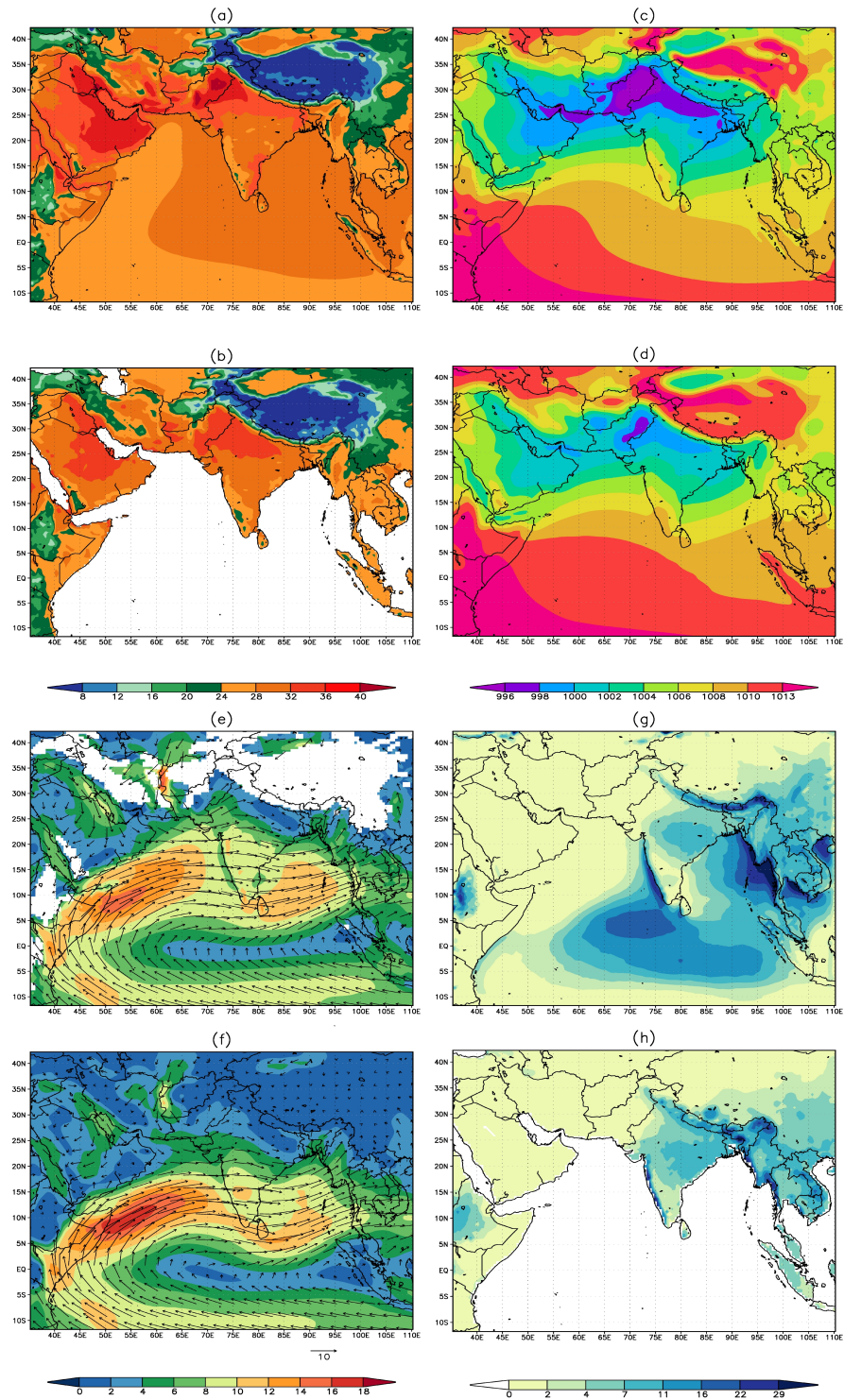


Figure 2.3: Summer (JJAS) climatologies (1961–2000) of 2m temperature ($^{\circ}\text{C}$) (a) REMO, (b) CRU observations; mean sea level pressure (hPa) (c) REMO, (d) ERA40 reanalysis; 850 hPa winds (m/sec) (e) REMO, (f) ERA40 reanalysis; and precipitation (mm/day) (g) REMO, (h) Willmott and Matsuura observations.

case however, the excess of differential heating between land and sea has given the active role to the westerlies to intrude inside the central India throughout the monsoon season. This causes a situation unfavorable for westward propagating currents from BOB to intrude deep into western India and Pakistan. Therefore, less moisture is advected causing an underestimation of precipitation over this area (Figures 2.1(g) and (h)).

In his study of SASM with the General Circulation Model ECHAM4, May (2003) found a similar warm bias over Indus basin, and suggested that it was because of an unrealistic drying of the soil during the dry season (boreal winter and spring) due to the model's limited capacity of storing water in the ground. This leads to a reduction of evaporation and hence would reduce the local production of precipitation during the wet season. However in REMO, there is increased soil water storage capacity as compared to ECHAM4, and similar behavior of REMO leads to rejection of this hypothesis (Hagemann et al., 1999). Although REMO and ECHAM4 have different physics and dynamics than RegCM3, similar overestimation of temperature over the same region is found in the simulation of SASM using RegCM3 (Ashfaq et al., 2009). This similar bias in different models forces us to believe that a characteristic process of the region might be missing in all these models.

2.4 REMO-Irrigation

As mentioned above, the largest positive temperature bias simulated by REMO is confined to highly irrigated basins of the Indian subcontinent. In the REMO-baseline experiment, simulated surface runoff and drainage account for 45% of the total precipitation falling over Indus basin, which is much larger than the observed value of 14% (Karim and Veizer, 2002). This means that REMO simulates extra $\sim 30\%$ of precipitation entering runoff instead of ET. This excess water is lost from the model, as in REMO and almost in all regional models, the lateral surface runoff and drainage generated in each time step are removed from the simulated water cycle due to the absence of any routing and irrigation schemes. The removal of this water in REMO results in the underestimation of ET that accounts for only 55% of total precipitation compared to the observed value of 84% (Karim and Veizer, 2002). Consequently, this leads to a reduction of local precipitation as proposed by May (2003). When irrigation is accounted for, a more realistic behavior of the simulated climate is yielded. Figure 2.4 compares the changes simulated by REMO-irrigation with the REMO-baseline run for the period 1989-1992. Improvement in temperature and MSLP can be seen all over the domain, but statistically significant and most pronounced changes are present over Indus, Ganges and southern India (Figures 2.4(a) and (b)). It can be noticed that these changes have occurred over the regions where there was an acute bias before (Figures 2.3(a) to (d)), hence showing better representation of these variables. Figure 2.4(c) indicates significant increase in ET over the whole subcontinent region, again with largest increase over Indus and southern India. The ERA40 ET is also model generated; yet it shows realistic patterns with higher values over Indian subcontinent than over the drier region in the western

2 Impact of irrigation on South Asian summer monsoon

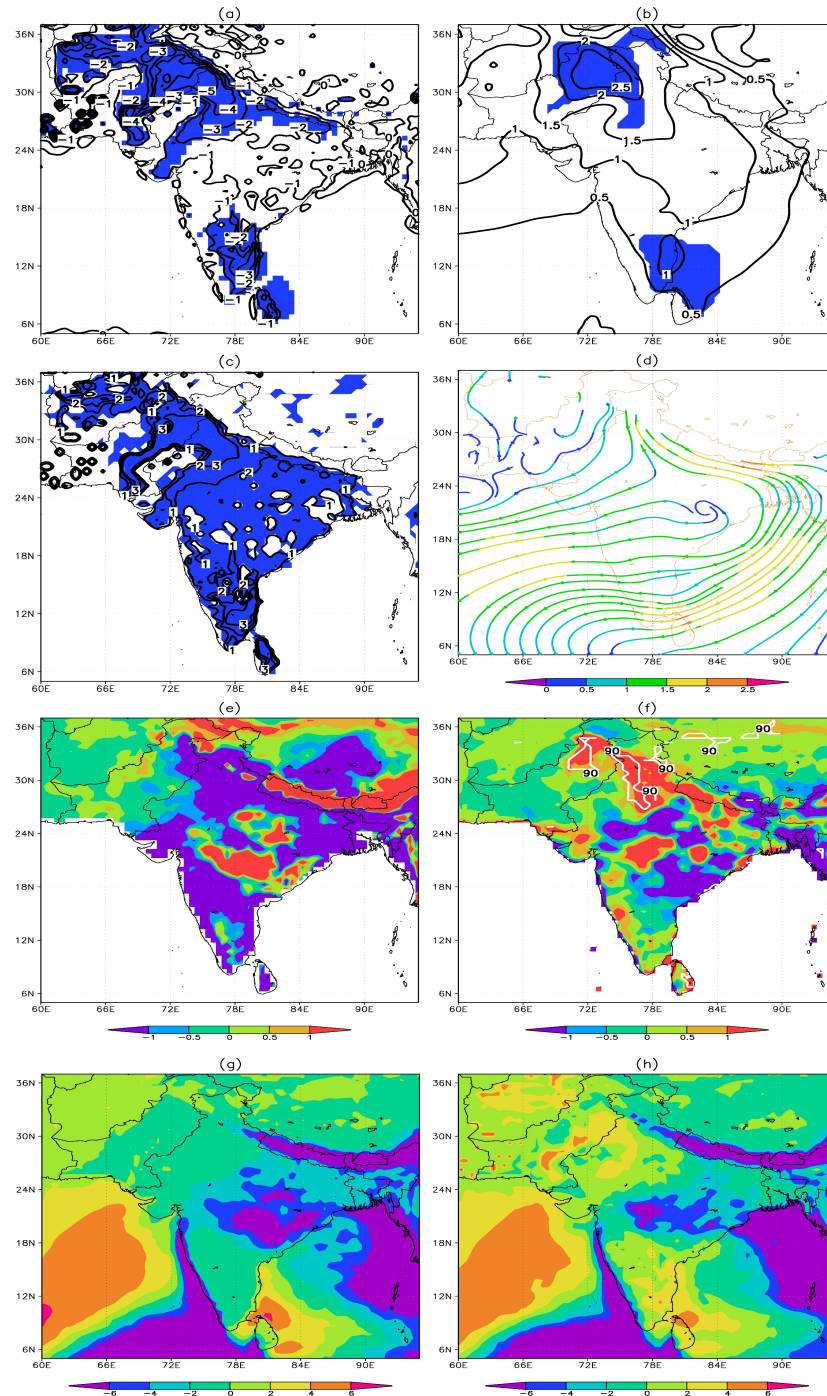


Figure 2.4: Simulated summer (JJAS) averages for 1989–1992 zoomed over the Indian subcontinent. Difference (REMO-irrigation minus REMO-baseline) of (a) 2m temperature ($^{\circ}\text{C}$), (b) Mean Sea Level Pressure (hPa), (c) Evapotranspiration (mm/day), (d) 850 hPa winds; shaded blue area represent significance at 90 percent from two tailed t-test. Precipitation (mm/day) differences of (e) REMO-baseline minus WM, and (f) REMO-irrigation minus REMO-baseline with areas significant at 90 percent level are shown by closed polygons. Simulated convergence (mm/day) of (g) REMO-baseline, and (h) REMO-irrigation.

part of the domain, whereas REMO-baseline does not show a realistic simulation of ET with very low values over the highly irrigated Indian subcontinent especially over the Indus basin (Figure 2.5). In our REMO-irrigation experiment, the introduction of water on the irrigated grids has caused the pattern of ET quite similar to that of ERA40, and over the four years period from 1989–1992 the correlation over land points between REMO-irrigation and ERA40 is increased to ~ 0.88 as compared to the correlation between REMO-baseline and ERA40 of ~ 0.83 . REMO-baseline simulated ET is $\sim 52\%$ of the total precipitation over the Indus basin, which was quite lower than the long term observed value of 84% (Karim and Veizer, 2002). However in the REMO-irrigation experiment, the value of ET is $\sim 92\%$ of the total precipitation which is not unrealistic as compared to 84% of the observed value. Here, an overestimation could be expected as the REMO-irrigation experiment assumes optimal irrigation conditions. The wind pattern shows complex behavior with less flow towards the foothills of Himalaya and into Ganges and Indus basin. However, from central India downwards, the decrease in westerly winds from the Arabian Sea into the Indian plains is also reduced due to the reduction of land sea differential heating (Figure 2.4(d)). The only significant change in precipitation is the increase in the western-northwestern India and Pakistan (Indus and Ganges basins), which is attributed to the local recycling of water, also shown in the convergence plot (Figures 2.4(g) and (h)). Convergence C of vertically integrated water vapor flux in a grid box is calculated from the water vapor conservation equation (Peixoto and Oort, 1984).

$$C = ET - P - \Delta S \quad (2.1)$$

where ET and P are evapotranspiration and precipitation respectively, and ΔS is the change of vertically integrated specific humidity during each 6 hourly time step. Here the positive values will represent divergence and negative values will show convergence of water vapor in a grid box. From Figures 2.4(g) and (h), the net divergence of moisture from western India and Pakistan area in REMO-irrigation as opposed to net convergence in REMO-baseline can be noticed. This indicates the increased contribution of evapotranspiration in providing increased amount of moisture for precipitation, hence causing local recycling. In central India, the REMO-irrigation has reduced the precipitation's wet bias near the BOB coast and is producing more precipitation further inland. This behavior can also be seen in convergence plots where the convergence is reduced in the region near the BOB and a convergence maximum is formed west of 78° E. As mentioned before that due to the reduced westerlies (Figure 2.4(d)) there is more chance for the monsoon currents, in the form of depressions/lows (Ds/Ls) and cyclones originating from BOB, to intrude deep into land in REMO-irrigation. Under normal circumstances, these currents play a vital role in distribution of rainfall during SASM. Whereas in REMO-baseline, the precipitation wet bias near BOB over central India is because of the blocking effect of westerlies, limiting the movement of westward propagating monsoon currents. This leads Ds/Ls and cyclones to deposit their moisture over coastal areas without intruding deep inside the land.

To further ascertain our findings, examples of the development and movement of mon-

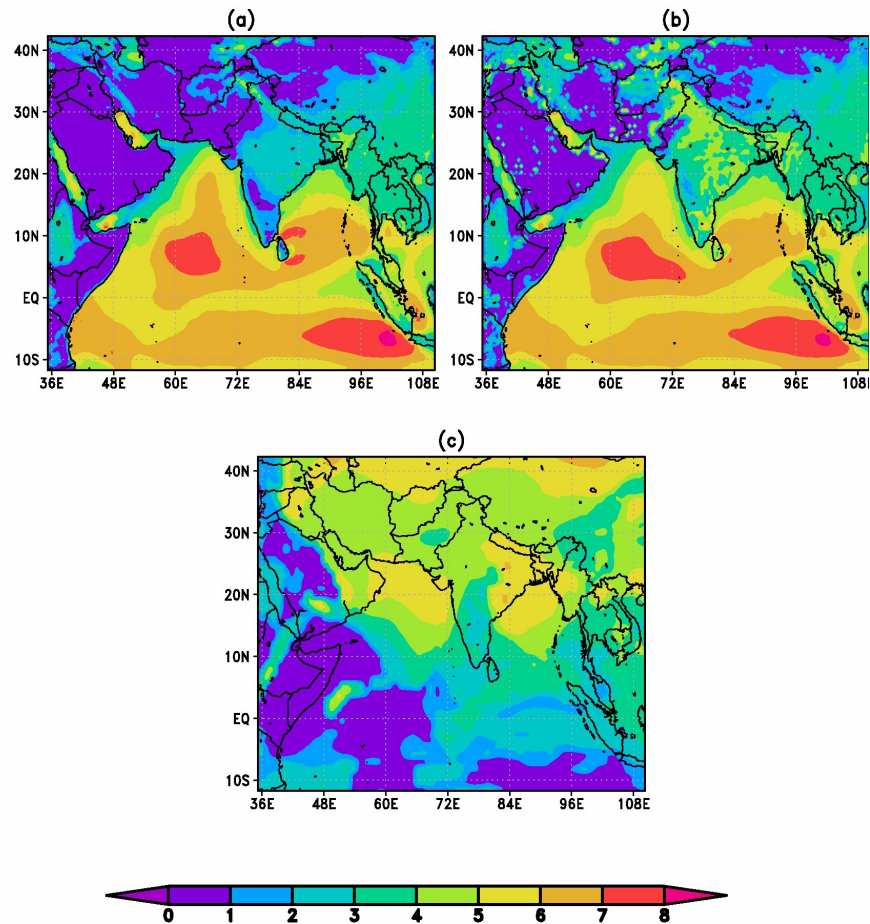


Figure 2.5: Four years simulation results of evapotranspiration (mm/day) (a)REMO-baseline, (b)REMO-irrigation, and (c)ERA40.

soon Ds/Ls are also considered (Figure 2.6). The criteria for selecting these examples is their occurrence in different months, should be captured by either of the simulation during the period 1989-1992 and discussed in earlier published literature (Mahajan et al., 1995; Narkhedkar et al., 1995; Seetaramayya et al., 1993). It is evident that the development of monsoon Ds/Ls is more pronounced in REMO-irrigation and travels deep into land towards western India and Pakistan in all events as compared to REMO-baseline. Moreover, in 23-27 July 1991, REMO-irrigation shows the development and inland movement of a depression, which is not even captured in the case of REMO-baseline. Therefore, the increase in precipitation in central/western India and Pakistan is not only attributed to the local recycling of moisture, but also to the currents from BOB penetrating into these areas.

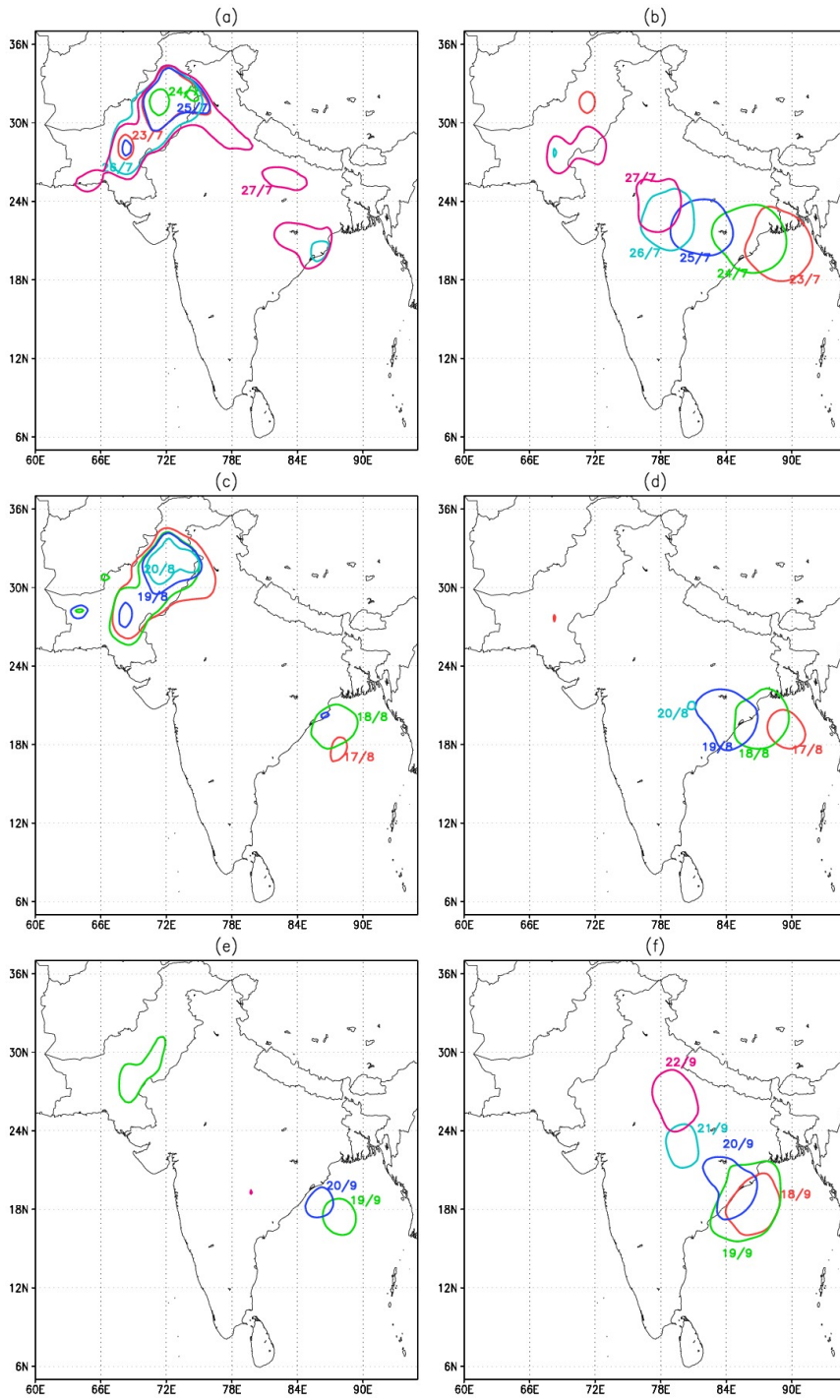


Figure 2.6: Monsoon depressions/lows development and movement: July 23–27, 1991 at 993 hPa MSLP (a) REMO-baseline (b) REMO-irrigation; Aug 17–20, 1990 at 996 hPa MSLP (c) REMO-baseline (d) REMO-irrigation; and Sep 18–22, 1991 at 999 hPa MSLP (e) REMO-baseline (f) REMO-irrigation.

2.5 Conclusions

The present study signifies the role of irrigation in effecting the local temperature, which in turn effects large-scale circulations and precipitation. It is also mandatory to consider the irrigation over Indus Basin while analyzing effects of irrigation on SASM, which was missing in earlier studies. It may be concluded that representation of water used for irrigation is unavoidable for the realistic simulation of SASM circulation and associated rainfall in climate models. This study has also pointed out the conclusion of May (2003), which criticizes the use of the simple so-called bucket scheme and highlights a need for more sophisticated parameterization of land-surface hydrology of the model, in order to remove the temperature bias. In contrast, it has been shown that the non-representation of irrigation water is the root cause of this overestimation rather than the simple treatment of soil hydrology in the model.

Results indicate that representation of irrigation has caused the removal of the warm bias and overestimation of the monsoon heat low. This has not only resulted in increased evapotranspiration effecting vertical exchanges and causing local production of precipitation, but also the reduction of the heat low has caused less westerlies to enter into land from Arabian Sea. This reduction of westerlies over land has created favorable conditions for currents from BOB to intrude deep into land, thereby removing the precipitation wet bias near BOB coastal area and dry bias over central/western India and Pakistan.

80% of Indus basin river flows are attributed to the melt of snow and glacier. Considering the large impact of irrigation on SASM behavior, one can assume that under global warming the changes in the timings of water inflows would shift towards earlier months, hence causing changes in cropping patterns and subsequently irrigation. It may also be concluded that the changes in irrigation patterns over the Indus basin may have a substantial effect on SASM circulation and associated rainfall under climate change.

3 A framework for the evaluation of the South Asian summer monsoon in a regional climate model applied to REMO

3.1 Introduction

With the dependence of a large percentage of world's population on its annual rainfall, the South Asian summer monsoon (SASM) has been the subject of numerous scientific studies since long. For a couple of centuries, scientists have been trying to discover the factors that influence the SASM system. Initial work on SASM by Edmond Halley in 1686, H. F. Blanford in 1877 and Sir Gilbert Walker in 1904 (Katz, 2002; Kripalani et al., 2007; Mohanty et al., 2007) set the tone for further research in the coming centuries. Because of its 'notoriously difficult to predict nature' (Jayaraman, 2005), SASM poses challenges to scientific community working over the region even at present times.

Today, coupled atmosphere ocean general circulation models (AOGCMs) are considered to be the most advanced numerical tools to carry out global climate simulations. The general circulation of the atmosphere, which is driven by large-scale climatic forcing, can be effectively simulated by AOGCMs. The typical horizontal resolution of AOGCMs is about 200–300 km, and many regional-scale climatic processes go beyond the scope of AOGCMs. For this reason, the nested regional climate modelling technique was developed to downscale the AOGCM results to the regional scale, and thus these models are called Regional Climate Models (RCMs).

The past decade has witnessed a rapid growth in the development and application of RCMs. By simulating the climate at a limited model domain, the higher-resolution simulations have become computationally less expensive than AOGCMs. RCMs now run on a grid size between 50 and 10 km and on time scales up to 150 years (Jacob, 2008; Jacob et al., 2007). Today, this technique is becoming popular among the developing countries as well (Pal et al., 2007). A brief review of regional climate modelling, from its ensuing stages in the late 1980s to the recent past can be found in Giorgi (2006).

The simulation of the South Asian summer monsoon, which extends from Tibet to the southern Indian Ocean, and from East Africa to Malaysia, has been a focus in meteorological research due to its complex mechanism. In the past, there have been attempts to capture monsoon features with RCMs on a shorter time scale of up to a

few years (Bhaskar Rao et al., 2004; Bhaskaran et al., 1996; Dash et al., 2006; Ji and Vernekar, 1997; Patra et al., 2000; Singh et al., 2007). More recently, Dobler and Ahrens (2010) conducted a comprehensive study on the analysis of the regional model ‘COSMO-CLM’ forced by reanalysis data and a GCM. Regional models have also been used to study the long-term effects of climate change due to enhanced greenhouse gases over South Asia (Ashfaq et al., 2009; Kumar et al., 2006). Most of the above mentioned studies are either restricted to very short time periods of a couple of seasons or lacking in the rigorous evaluation of the model when forced with reanalysis data over a longer time scale of 30 or more years which is a typical time scale for climate studies.

RCM of the Max Planck Institute for Meteorology, the REgional MOdel (REMO; Jacob (2001)) has been used widely for various studies in many parts of the world (e.g. Europe (Jacob et al., 2007); South America (Silvestri et al., 2009); South Africa (Haensler et al., 2010)), however, it has not been extensively tested over the South Asian sub-continent monsoon region. Although, in the second chapter of this thesis the REMO results have been presented over the SASM domain with the prime focus on identifying the effects of irrigation on SASM circulations and associated rainfall. The second chapter has evaluated the performance of REMO over SASM region rather briefly and it was restricted to surface variables such as temperature, mean sea level pressure, precipitation and low-level winds. Considering the complexities and deep vertical structure associated with the SASM system, there is a need to evaluate these results in much more detail. Usually, the analyses of RCM applications focus on surface parameters, thereby often neglecting the origin of biases in these parameters. However, if it can be shown that a RCM is able to capture the fundamental structure of SASM, then biases in surface variables can be attributed to deficiencies in model parameterizations or missing processes.

In the present study, an evaluation framework for the representation of SASM circulation and associated rainfall is presented. The performance of REMO in simulating SASM features is rigorously evaluated over a 40-year time scale using the recent REMO version, which we think was missing in earlier studies done by different RCMs over this region. Such a validation is necessary for gaining the confidence in RCM, in this case REMO, to carry out in-depth studies such as climate change and its probable impacts over the region. A brief description of REMO and experiment design is given in Section 3.2, and in Section 3.3 the evaluation framework for validation of model is introduced. Section 3.4 deals with the simulation results and final considerations are presented in Section 3.5.

3.2 Model and experimental setup

The regional climate model REMO is based on the Europamodell/Deutschlandmodell system (Majewski and Schrodin, 1994). It uses a modified version of the physical parameterization package from the general circulation model ECHAM4 (Roeckner et al., 1996). A linear fourth-order horizontal diffusion scheme is applied to momentum, temperature, and humidity. The finite difference equations are solved on an Arakawa-C grid.

At the lateral boundaries of the model domain, a relaxation scheme according to Davies (1976) is applied, which adjusts the prognostic variables in a boundary zone of eight grid boxes calculated separately for the different compartments within a model gridbox (Semmler et al., 2004). The vegetation-dependent land-surface parameters are taken from the LSP2 dataset (Hagemann, 2002), and monthly variations are implemented by Rechid and Jacob (2006) (leaf area index, vegetation ratio) and Rechid et al. (2009) (surface background albedo). In REMO, the improved Arno scheme (Hagemann and Gates, 2003) is implemented to represent the separation of rainfall and snowmelt into surface runoff and infiltration.

REMO has been applied at a resolution of 0.5° (~ 55 km) over the South Asian domain which encompasses 12°S to 42°N and 35°E to 110°E with 109 grid points along the latitudinal and 151 grid points along the longitudinal direction. A continuous simulation is made for the years 1961–2000 with 3 years of spin-up from 1958–1960. The model is forced with so-called perfect lateral boundary conditions at a resolution of 1.125° , obtained from the European Centre for Medium-Range Weather Forecasts (ECMWF) 40-year reanalysis (ERA40; Uppala et al. (2005)).

3.3 Evaluation framework

As mentioned earlier, second chapter of this thesis briefly described an initial evaluation of REMO over SASM, which was limited to only a few surface and near-surface variables. Therefore, readers are advised to see the performance of variables such as 2 m temperature, mean sea level pressure, etc. in second chapter. But these variables may not be the true representatives of the complex SASM system, because some of these variables (such as precipitation) are modelled very late in the process chain of climate models. There are also other processes, such as irrigation, as mentioned in the second chapter, which are not represented in these models. Therefore, conclusions based on these results may be misleading unless special consideration is given to the performance of the model in capturing the fundamental structure of SASM system. Here we will focus more on the SASM circulation, its associated indices and other features that are better representatives of the complex spatial and deep vertical structure of the SASM system.

O’Hare (1997) in his explanation of the SASM highlighted the importance of deep vertical structure of SASM circulation. According to him, the differential heating between land and ocean creates a pressure gradient from ocean to land at the surface level even in the pre-monsoon months of April in May. However, rising air over hot land surface creates high pressure aloft in the middle troposphere only up to the height of around 6–7 km, resulting in another pressure gradient from land to ocean. Since the upper tropospheric component remains from ocean to land, the complete monsoon circulation does not become obvious in pre-monsoon months of April and May. In the active monsoon months of June to September, in addition to the lower and middle tropospheric circulation, the high land of Tibet having average height of 4000 m produces strong sensible and latent heat fluxes resulting in the development of a high-level anticyclone. This

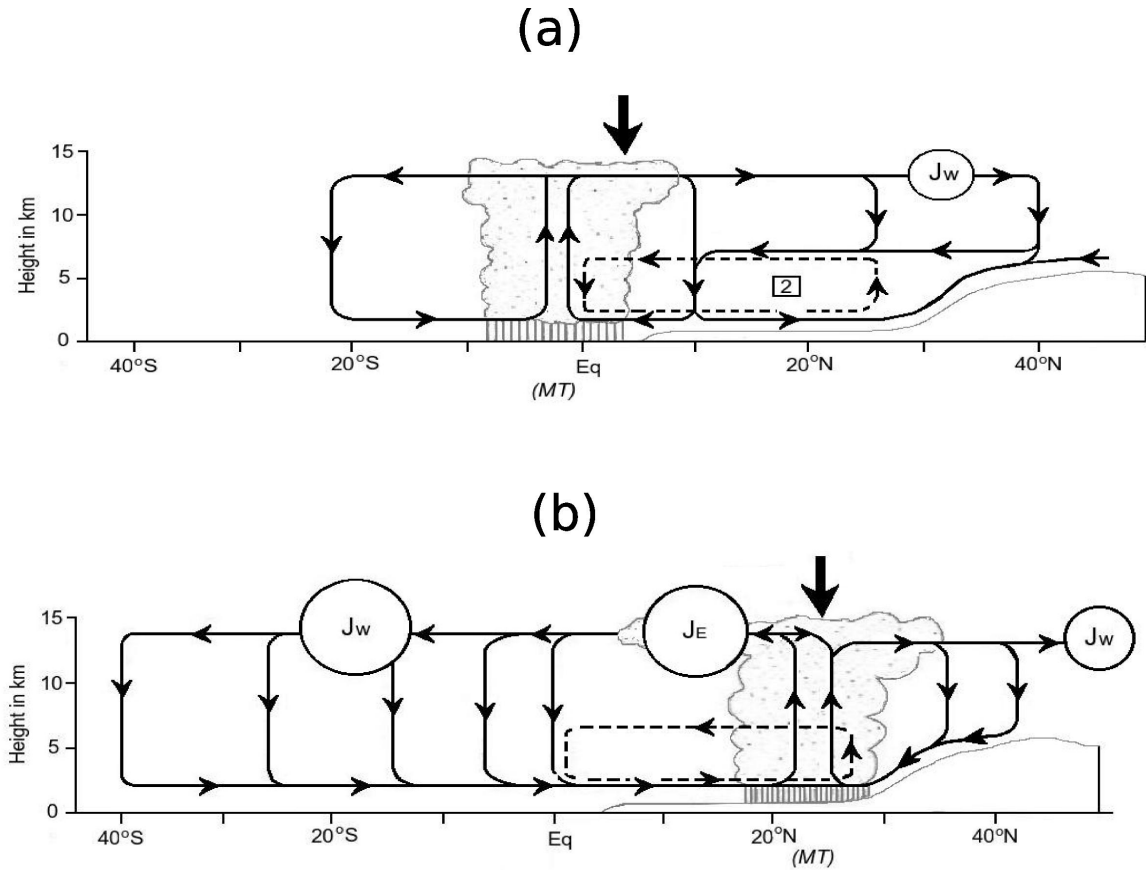


Figure 3.1: North to south vertical transect of the Indian monsoon circulation concept after O’Hare (1997). The westerly jet (J_W) moves ‘out of the paper’ while the easterly jet stream (J_E) moves ‘into the paper’. Two monsoon phases are shown (a) April to May (pre monsoon); (b) June to September (active summer monsoon). The vertical arrow indicates the mean position of the sun.

high-level anticyclone produces upper atmospheric easterlies, which causes an upper tropospheric circulation from land to ocean that was absent in earlier pre-monsoon months. Therefore, in monsoon months, an ocean-to-land component in the lower troposphere and land-to-ocean component in the middle and upper troposphere are observed. The schematic diagram of O’Hare’s concept is presented in Figure 3.1.

Over the past years, several monsoon indices have been developed in order to understand, measure, and predict the strength of SASM, as well as for the evaluation of climate models. A brief review of these indices can be found in Wang and Fan (1999). Following Parthasarathy et al. (1992) and Goswami et al. (1999), we have defined the Indian Monsoon Rainfall (IMR) and Extended Indian Monsoon Rainfall (EIMR) indices as the departure of rainfall from the climatological mean, averaged over 70°–90°E; 5°–25°N (land points only) and 70°–106°E; 10°–30°N, respectively. Basing on Webster and Yang (1992), an index (WY) has been defined as $U^*850 - U^*200$, where U^*850 and U^*200 are zonal wind anomalies at 850 hPa and 200 hPa respectively, averaged over the

region 40°–106°E; 0°–20°N. Similarly, basing on Goswami et al. (1999), we have defined the local Monsoon Hadley (MH) index as $V^*850 - V^*200$, where V^*850 and V^*200 are meridional wind anomalies at 850 hPa and 200 hPa respectively, averaged over the region 70°–106°E; 10°–30°N.

The shift of the Intertropical Convergence Zone (ITCZ) or monsoon trough (MT) from the equator to the SASM region is also studied at each grid point on a monthly basis. Two criteria are defined based on precipitation and vertical velocity. For precipitation, the threshold of 6 mm/day is considered after Gadgil and Sajani (1998) (GSI), which means that if this threshold is attained for a particular grid point in a particular month, we assume the appearance of the ITCZ in the respective grid point and month. We have also considered vertical velocity (VVI) to be a proxy for the ITCZ, since an upward motion is associated with the ITCZ. Therefore, we have defined the criterion that if on all pressure levels (taken to be 925, 850, 775, 700, 600, 500, 400, 300, 200, 100 hPa), a positive (upward) vertical velocity is occurring for a particular grid point in a particular month, we assume the appearance of ITCZ in the respective grid point and month.

The onset of the monsoon has been defined after Wang and LinHo (2002) and He et al. (2003). Following Wang and LinHo (2002) (WLO), the climatological monsoon onset at each grid point is defined as the first pentad (five-day mean) in which the climatological mean precipitation exceeds five mm/day and the grid-point January mean. Following He et al. (2003) (HSO), the onset can be defined according to the following relationship

$$I_{wh} = I_w \cdot \frac{I_h}{|I_h|} ; \text{ when } I_w > 0, \text{ otherwise } I_{wh} = I_w \quad (3.1)$$

where;

$$I_w = I_u \cdot \frac{V_{850}}{|V_{850}|}, I_h = H_s - H_n \text{ and } I_u = U_{850} - U_{200}$$

Here, U_{850} and U_{200} are mean zonal wind at 850 and 200 hPa, V_{850} the regional mean meridional wind at 850 hPa and $|V_{850}|$ represents the absolute value of V_{850} . I_u is calculated over the region 40°–110°E; 0°–20°N, whereas V_{850} is taken over the region 50°–85°E; 5°N–20°N and $H_s - H_n$ is the 850 hPa geopotential height difference between two selected points at (70°E, 5°N) and (50°E, 20°N).

The meridional tropospheric temperature gradient (MTG) has been defined after Webster et al. (1998), as the difference of the five-day climatological mean temperature between the upper tropospheric layers (200 hPa –500 hPa) at 30°N and 5°N, averaged over the zonal belt between 50°E and 85°E. Following Li and Yanai (1996), we calculated the easterly vertical shear of zonal winds (ESZW) as the difference of the five-day climatological mean of zonal winds between 200 hPa and 850 hPa averaged over the region 50°E–90°E; 0°–15°N.

In the second chapter, simulated surface variables were mainly compared to observed datasets. Since the present study is focusing more on the vertical structure of SASM, we are validating the model results against reanalysis datasets. Although they have some caveats due to modelling limitations, reanalysis datasets are representing the current climate better than any other model due to their assimilation of observations. In this

study, we focused mainly on the validation of model against ERA40 reanalysis, however, for the computation of index correlation we have also considered the National Centers for Environmental Prediction/National Center for Atmospheric Research (NCEP/NCAR) reanalysis (Kalnay et al., 1996).

3.4 Results

In this section the results of our analysis of the different SASM indices are shown and discussed.

3.4.1 Winds

First the simulated wind flow at 850 hPa and 200 hPa, along with ERA40 data is shown in Figure 3.2. The regional characteristic features of the lower troposphere such as cyclonic flow pattern over the Bay of Bengal, cross-equatorial flow near the African coast forming the low-level jet stream called Somali jet that is an important mechanism in transferring heat and moisture to the subcontinent (Halpern and Woiceshyn, 1999), and westerly flow over northern Arabian Sea and India are captured reasonably well by REMO (Figure 3.2(a)) compared to ERA40 (Figure 3.2(b)).

Apparently, REMO realistically simulates the general structure of the lower tropospheric circulation, however, some discrepancies are also present. It can be noticed that although the location of the core of the Somali jet is well simulated, its strength is rather underestimated compared to ERA40. In the same way, the wind speeds over the northern Arabian Sea entering into India and Pakistan are overestimated. In second chapter, it was suggested that this behaviour is caused by deficits in the simulation of 2 m temperature and mean sea level pressure due to the absence of an irrigation scheme in REMO. The erroneous intensification of the heat low causes an intense pressure gradient in the south north direction over the Arabian sea, overpowering the coriolis force, and hence, drawing more winds with higher wind speeds into the land areas as westerlies. However, it should also be noted that a significant difference between the reanalysis products exists for this region. For example, Annamalai et al. (1999) found differences in the strength of the Somali jet between ECMWF and NCEP/NCAR reanalysis of up to 5 m/s, as well as differences in the pattern of flow over the Indian peninsula and over the Indian Ocean. Considering the flow field at 200 hPa in Figure 3.2 (c) and (d), the major discrepancy between REMO and ERA40 is the overestimation of westerly winds in the northern part of the domain. Other than that, the model has ably captured the Tibet anticyclone as well as the strength and the direction of the upper tropospheric easterlies.

Figure 3.3 is used to investigate whether O Hare's concept of three components SASM circulation can be reproduced by REMO. It can be seen that in the pre-monsoon period of April and May, the lower troposphere ocean-to-land, the middle troposphere land-to-ocean, and upper troposphere ocean-to-land component is simulated quite well by REMO (Figure 3.3(a)) in comparison with ERA40 (Figure 3.3(b)), and the structure

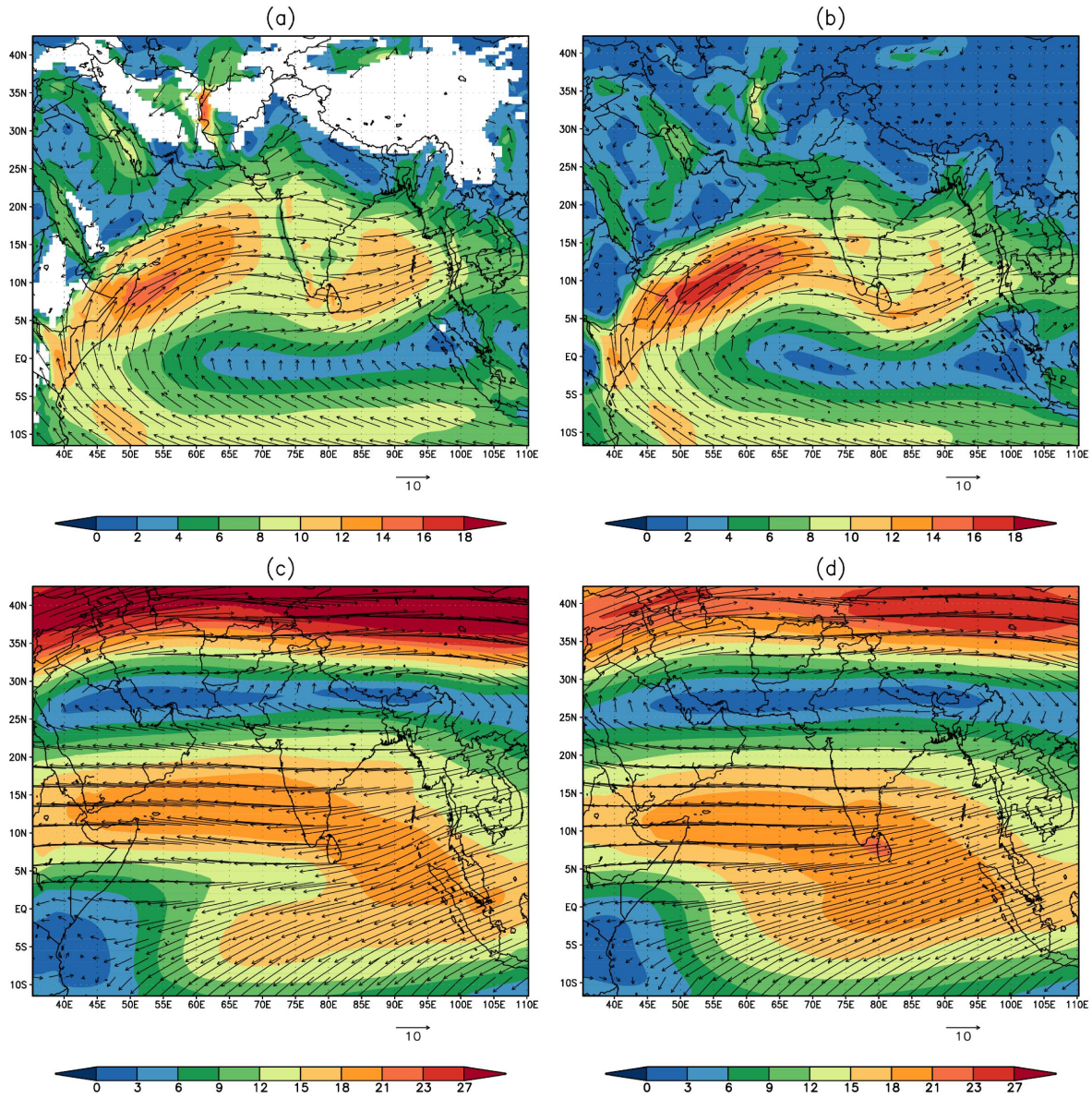


Figure 3.2: Mean summer (JJAS) average wind (m/s) at 850 hPa. (a) REMO (b) ERA40; and at 200 hPa. (c) REMO (d) ERA40.

is in line with the description given in Figure 3.1(a). However, in the active monsoon period of June to September, the lower and middle tropospheric components are slightly overestimated by REMO (Figure 3.3(c)) in comparison to ERA40 (Figure 3.3(d)). It should be noted that only the meridional wind component is shown, thus, the strong upper tropospheric component from land to ocean is not obvious here. The reason for this is that winds associated with the Tibetan anticyclone have a strong zonal component, which overpowers the meridional component in the northern part of the domain. However, in the southern part, a noticeable upper tropospheric land-to-ocean component

3 A framework for the evaluation of SASM applied to REMO

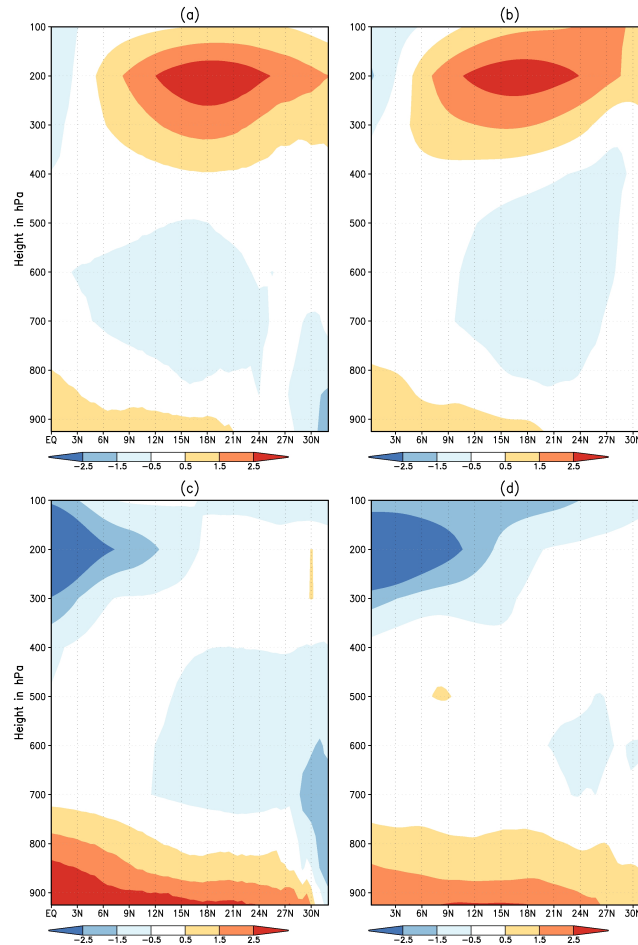


Figure 3.3: North to south vertical transect of the Indian monsoon circulation over the region 60° - 105° E, 0° - 32° N reflected by the meridional (v) wind component (m/s) for April-May (pre monsoon) (a) REMO (b) ERA40; and for June to September (active summer monsoon) (c) REMO (d) ERA40

exists in both REMO (Figure 3.3(c)) and ERA40 (Figure 3.3(d)), representing easterlies associated with the Tibetan anticyclone.

3.4.2 Correlation between precipitation and circulation indices

Goswami et al. (1999) defined a new index for precipitation (EIMR) on a broader region including Bay of Bengal and land masses of Myanmar, Thailand and parts of China, as compared to previously recognized IMR index, which was defined only over the land mass of India. They argued that the large precipitation over the Bay of Bengal having significant interannual variability cannot be ignored in the definition of SASM, and hence, EIMR is a better indicator of convective heating fluctuations associated with the SASM than IMR.

(A)				
INDEX	IMR	EIMR	MH	WY
IMR	1			
EIMR	0.72	1		
MH	0.66	0.73	1	
WY	0.67	0.61	0.63	1

(B)				
INDEX	IMR	EIMR	MH	WY
IMR	1			
EIMR	0.92	1		
MH	0.40	0.46	1	
WY	0.26	0.27	0.39	1

(C)				
INDEX	IMR	EIMR	MH	WY
IMR	1			
EIMR	0.82	1		
MH	0.65	0.58	1	
WY	0.51	0.40	0.48	1

Table 3.1: Cross-correlation among different indices for: (A) REMO; (B) ERA40; (C) NCEP

In order to reflect the variation of monsoon heating, Webster and Yang (1992) defined a broad-scale circulation index WY, however Goswami et al. (1999) argued that WY index has little correlation with IMR and EIMR. Therefore, they have also identified a circulation index (MH) describing it as better representative of interannual variability of SASM as compared to the previous WY index. They established this by showing higher temporal correlations between MH index and precipitation indices as compared to WY index. The areas over which the IMR, EIMR, MH, and WY are defined are given in Section 3.3.

REMO shows higher correlations among most of the indices than the reanalysis datasets. Reanalysis being an assimilation product may have generated fields that may represent reality better than REMO due to the inclusion of observations, however, higher correlations among indices confirm the ability of REMO in capturing the dynamical link between them. The main conclusion of Goswami et al. (1999) that "... the MH index is significantly correlated with the EIMR", is very well indicated in Table 3.1 for the case of REMO. It can be seen that MH and EIMR has highest correlation for the case of REMO as compared to other indices, which is not found for both reanalysis datasets.

3 A framework for the evaluation of SASM applied to REMO

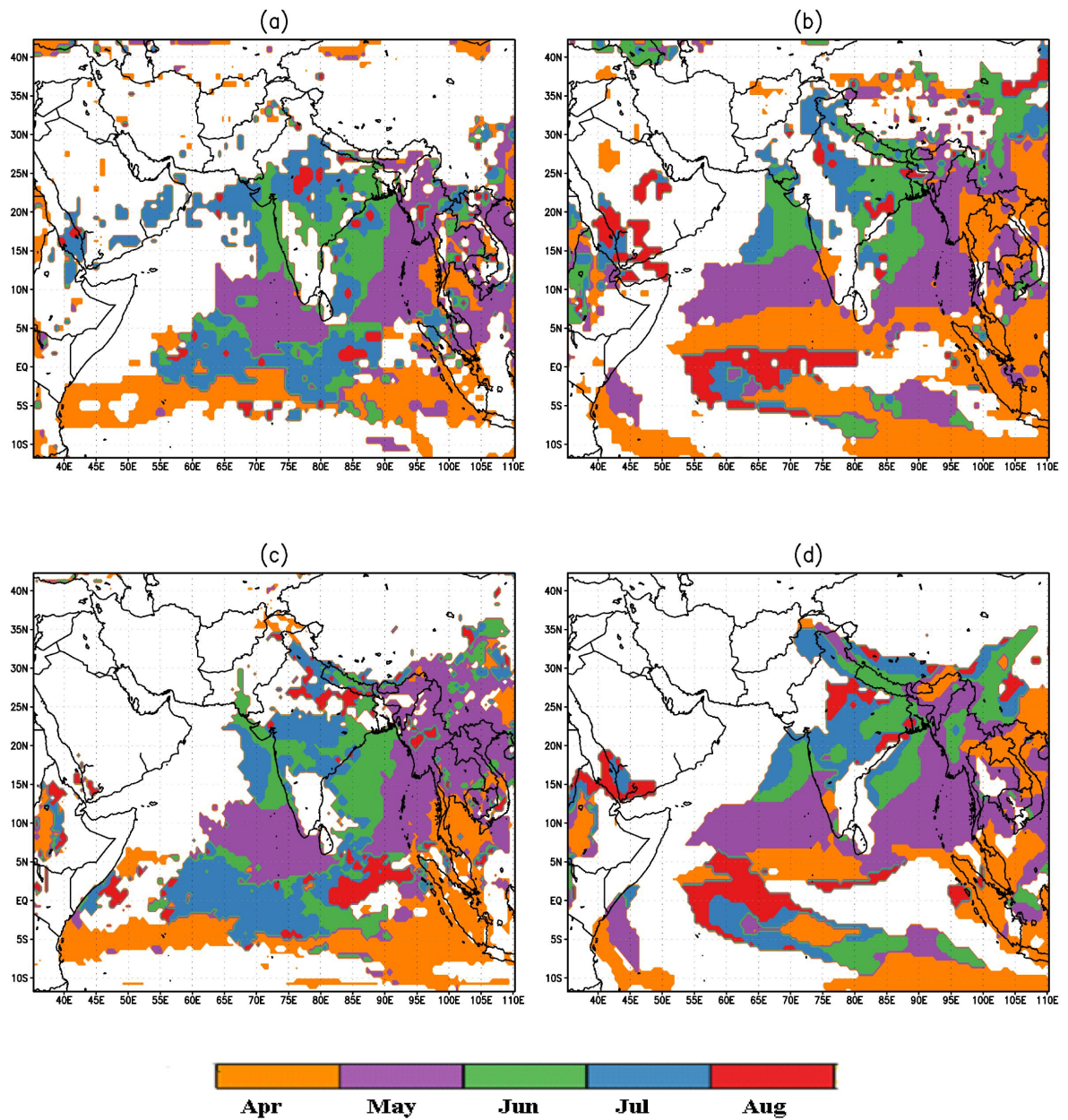


Figure 3.4: Monthly shift of ITCZ from April to August based on precipitation (GSI): (a) REMO (b) ERA40; and based on vertical velocity (VVI): (c) REMO (d) ERA40

Since REMO is forced by ERA40 data on its boundaries, therefore, this behaviour may be regarded as added value of the dynamical downscaling with REMO.

3.4.3 ITCZ indices

The monthly shift of the ITCZ, or sometime called as TCZ (Tropical Convergence Zone) is shown in Figure 3.4. The gradual northward shift of the ITCZ from the equator to northern latitudes during SASM is simulated reasonably well by REMO both for VVI (Figure 3.4(a) and (b)) and GSI (Figure 3.4(c) and (d)).

Another feature of the SASM, the generation of the second precipitation zone over the equatorial Indian Ocean on the intra-seasonal time scale has also been documented in earlier literature (Sikka and Gadgil, 1980). Following the criterion for ITCZ indices defined in Section 3.3, REMO has reproduced the development of a secondary ITCZ along the equator, generally one month earlier as compared to ERA40 for both VVI and GSI. This is probably due to the reason that REMO simulates a higher amount of precipitation over the ocean along the equator and less precipitation over northwest India and Pakistan as discussed in second chapter of this thesis.

3.4.4 Onset indices

The comparison of the simulated WLO index as compared to ERA40 data (Figure 3.5) indicates that REMO has successfully simulated the onset over the Arabian Sea and western India. However, the model has simulated the onset one pentad too late over eastern and central India, whereas over the foothills of the Himalayas the onset is too early. Again, this behaviour may be attributed to the overestimation of the heat low, as described in second chapter, retarding the movement of westward-propagating cyclones from the Bay of Bengal and bringing them towards the foothills of the Himalayas.

Similarly, Figure 3.6 shows the HSO index, where positive values of the curve represent the active monsoon. Although, the behaviour of the HSO index over the year is simulated very well by REMO, it has simulated the onset and withdrawal of the monsoon one pentad later and earlier, respectively, which means the simulated monsoon period is two pentads shorter than that of ERA40 if the HSO is considered. The results indicate that based on both the spatial (WLO) and temporal (HSO) indices, REMO has performed reasonably to capture the onset of the SASM.

3.4.5 MTG and ESZW indices

Finally, MTG and ESZW are considered in Figure 3.7. For MTG, the positive (negative) difference indicates that the upper tropospheric air is warmer (cooler) at 30°N than at 5°N , representing the reversal of MTG in the upper troposphere. Li and Yanai (1996) indicated that the positive reversal of the MTG is concurrent with the monsoon onset and produces zonal winds with easterly vertical shear as depicted by ESZW here. It can be seen that the simulated behaviour of MTG matches very well with that of ERA40, with concurrent positive phase from 32nd pentad to 54th pentad. For ESZW at some pentads, the difference between REMO and ERA40 has reached values as high as 4 m/sec. However, for most of the time in the positive phase of MTG, REMO simulated ESZW remains higher than the critical value of 20 m/sec as found by Goswami and

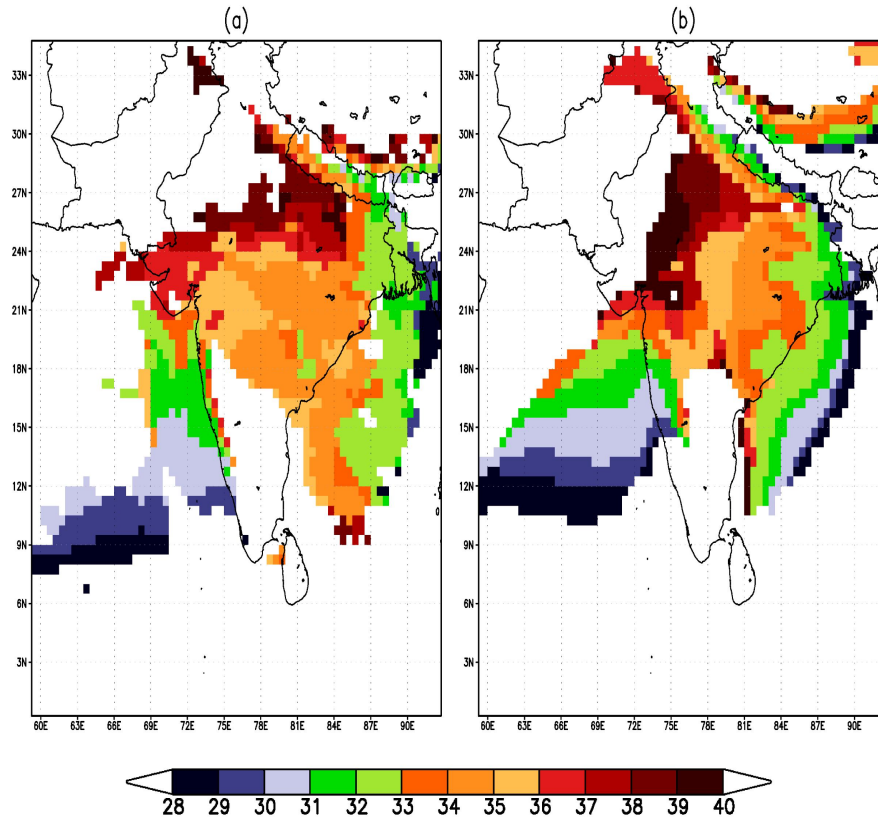


Figure 3.5: WLO Monsoon onset after Wang and LinHo (2002) (a) REMO (b) ERA40

Xavier (2005), indicating a satisfactory job done by REMO in simulating this behaviour.

3.5 Summary and conclusion

The South Asian region is considered to be one of the most challenging regions for the climate-modelling community due to its geography, orientation, population, and complexities of processes involved in the evolution of its climate. Within the present study, a regional climate simulation has been analysed and validated for the period 1961–2000. The simulation has been performed with the regional climate model REMO at a resolution of 0.5° driven by the ERA40 reanalysis at its lateral boundaries.

Precipitation (and other near surface variables) are modelled very late in the process chain in climate models and influenced by different processes, which are not represented in these models. Especially, the Indian subcontinent, which contains 22% of world’s population, has a strong feedback to the atmosphere through processes like irrigation. Therefore, comparison of just a few surface variables against observation is insufficient for the performance evaluation of a climate model especially over the SASM domain. In the present study, in order to gain the confidence in physics and dynamics of REMO, we

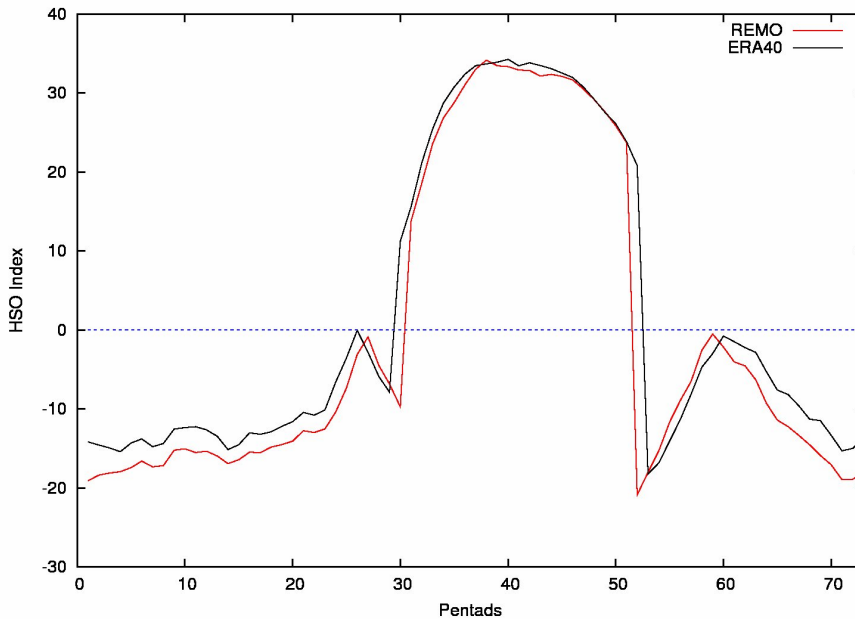


Figure 3.6: HSO monsoon onset index defined after He et al. (2003). The positive values of the curve represent the active monsoon period

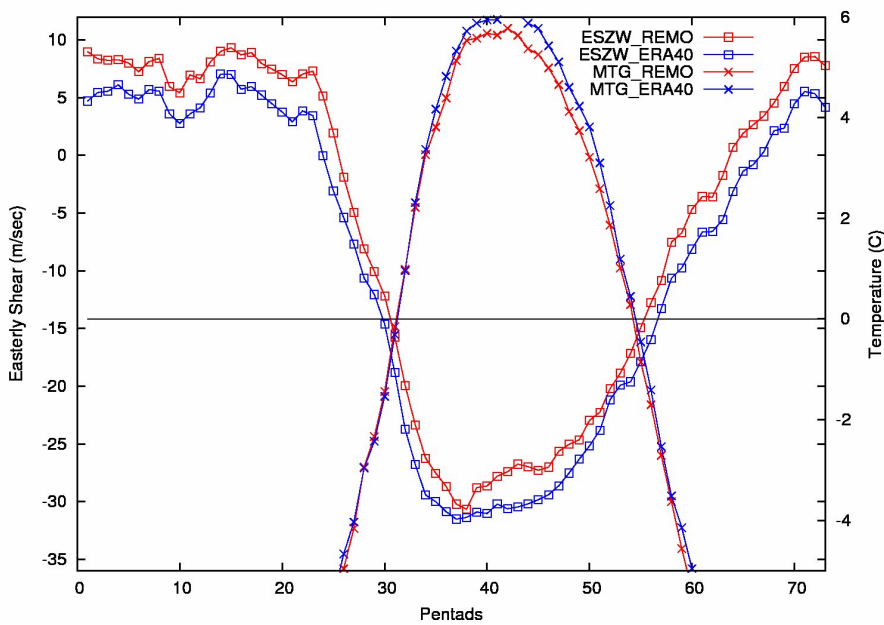


Figure 3.7: Easterly vertical shear of zonal winds (ESZW) and monsoon tropospheric gradient (MTG) following Li and Yanai (1996) and Webster et al. (1998), respectively. Horizontal black line represent 0 °C temperature

made an effort to evaluate how well the model is reproducing the basic structure of the monsoon circulation as explained in the theory. We have analysed different physically based indices, which have been used in the earlier literature to study the behaviour of SASM.

The model has successfully captured the patterns as well as the strength of the winds at different pressure levels. The location of the core of Somali jet is well simulated by the model with underestimated strength. On the other hand, the upper tropospheric circulations are also reasonably well simulated. Different components of SASM circulation, as defined by O'Hare (1997), of SASM circulation are also captured well by REMO. Seasonal shift of ITCZ, based on two criteria of precipitation and vertical velocity, is also simulated quite well by the model also showing the characteristic secondary ITCZ in the Indian Ocean. REMO shows high correlations between precipitation (EIMR) and circulation (MH) indices as identified by Goswami et al. (1999), adequately representing the dynamical link between them, which was missing for the case of reanalysis datasets showing low correlations between those indices. The onset of monsoon on a cohesive spatial-temporal scale shows a better agreement over the western part of the Indian peninsular, whereas, over the eastern part the onset is somewhat delayed. The model has done a satisfactory job in simulating the reversal of the meridional temperature gradient and easterly vertical wind shear, although the strength of the later is slightly underestimated throughout the year. The behaviour of the curve for He et al. (2003) onset index is also captured well by the model, however the length of the SASM season is squeezed by two pentads as compared to ERA40.

The application of the evaluation framework in the current study is the step forward to the earlier study done in the second chapter of this thesis, in which REMO was validated against the observations for near-surface variables, and an improvement of the results were shown due to the inclusion of irrigation representation. In this study, we have shown that REMO, even in its standard mode without irrigation representation, has the ability to reproduce the deep vertical structure and complexities involved in the SASM circulations. So far, to our knowledge, there have not been many studies available in which the rigorous evaluation of the regional climate model with reanalysis data over longer time scale is presented for the SASM region. We have proposed a comprehensive evaluation framework for the representation of SASM system based on different indices, which can prove to be very useful in gaining the confidence in the physics and dynamics of a regional climate model. Basing on the promising results presented in chapter 2 and the present study, we conclude that REMO is well suited to conduct a long-term high-resolution climate change projection for the SASM region. In future, this framework shall also be applied to other RCMs over the SASM region within the EU projects WATCH and HIGHNOON.

4 Influence of mid-latitude circulation on upper Indus basin precipitation: the explicit role of irrigation

4.1 Introduction

The economic life of Pakistan depends to a large extent on its agriculture, which in turn is dependent on irrigation through vast network of barrages, diversions and channels from the Indus river and its tributaries (Saeed et al., 2009b). Indus River rises on the Tibetan Plateau and in its passage through India and Pakistan, it drains the highest mountain ranges of the world. The basin is sometimes referred to as the “Third Pole” and contains the greatest area of perennial ice outside the Polar Regions ($> 20000 \text{ km}^2$) (Archer et al., 2010). Besides its importance for Pakistan, 9.85% of the total geographical area of India also lies inside Indus basin including Punjab, Haryana and Rajasthan which are the fertile granary of the country (Jain, S. K. and Agarwal, P. K. and Singh, V. P., 2007). Therefore, Indus river is a lifeline for large number of people living in that area.

Having a peculiar location, the Indus basin (Figure 4.1) receives precipitation in two distinct times of the year, namely winter (December to March) and summer (June to September), the latter is also known as South Asian Summer Monsoon (SASM). In the north of the basin, which comprises the trans-Himalayan Karakoram and Hindu Kush (HKH) ranges, precipitation primarily occurs as snow in winter and spring, resulting from westerly disturbances (Archer et al., 2010). However, considerable amounts of SASM rainfall are also received by the northern part during summer, especially on the southern slopes of Himalayan mountains. In summer season, the melt of glacier and snow that is accumulated during the preceding winter, along with monsoon rainfall leads to a peak in the annual discharge curve of Indus river and its tributaries. Although the northern part of Indus basin receive precipitation in both seasons, the southern half is considerably drier and depends on the water originating from the upper Indus Basin (UIB).

Considering the dependence of hundreds of million of people living on the Indus river, very little attention has been paid by researchers on UIB in contrast with rest of the Indian subcontinent. Main reasons for the lack of research in that area may be attributed to lack of observational data due to complex topography, challenging climatic conditions and also to some extent to the geopolitical situation of the region. Now with

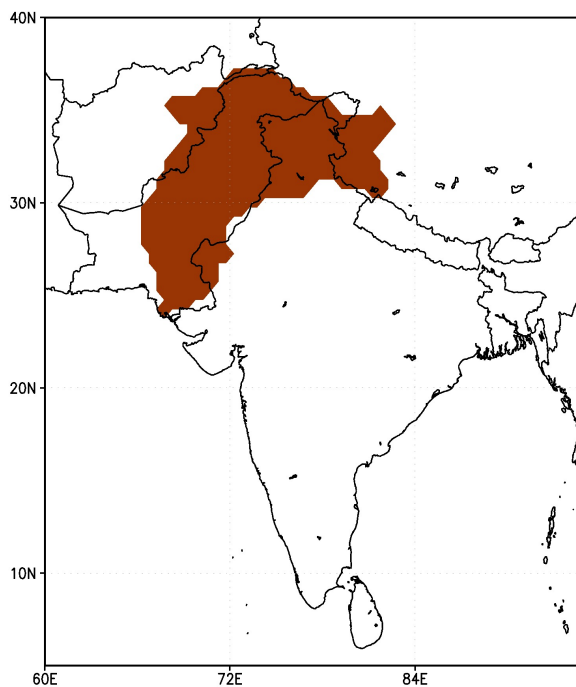


Figure 4.1: The mask of Indus Basin with rectangular area showing the extent of Upper Indus Basin (70° - 80° E, 30° - 36° N)

the easy availability of satellite data and reanalysis products, there have been a few studies recently conducted dealing with the winter precipitation on UIB (Syed et al., 2006; Yadav et al., 2010), however there has not been any such study for summer SASM precipitation. Although there are some studies focusing on isolated events over UIB, a comprehensive study dealing with the atmospheric situation that leads to precipitation is still missing for the region.

It has been well established that alongwith the surface and middle level, the upper level tropospheric features of the region also play a significant role in effecting the SASM precipitation, as for example the upper level 200 hPa Tibetan high (Hoskins, B. J. and Wang, B., 2005; Park et al., 1997; Yatagi et al., 1995). Similarly SASM undergoes enormous variability ranging from intraseasonal to interannual and decadal timescales, indicating the influence of tropical and extra-tropical processes (Goswami, 1998; Goswami and Mohan, 2001; Krishnamurthy and Goswami, 2000; Li et al., 2008; Shukla, J., 1987; Torrence and Webster, 1999). Several studies have noticed the potential influence of mid-latitude circulation on the SASM rainfall over the Indian region (Ding and Wang, 2007, 2005; Kripalani et al., 1997; Raman and Rao, 1981; Ramaswamy, 1962). Ding and Wang (2005) identified the mid-latitude circumglobal teleconnection (CGT) pattern (Branstator, 2002) also for the northern hemisphere summer. They showed that the monsoon activity over this region has a robust connection with the upper level anomalous high over central Asia. Furthermore, they proposed that the anomalous high over central Asia might enhance convection over northwestern India and Pakistan and hence the precipi-

tation. In recent studies, Yadav (2009) and Saeed et al. (2010) showed that the Rossby wave train over Eurasia is associated with intensifying the low surface pressure anomaly forming over Pakistan and adjoining areas of India, Iran and Afghanistan, which further intensifies the monsoon current over the Indian and Pakistan region.

Although there is an increasing evidence that there is an interaction between the mid-latitude circulation and intraseasonal variation of SASM over India, it is not fully understood that how the mid latitude circulation may influence the precipitation over UIB. The purpose of this study is to investigate the dominant weather characteristics associated with the midlatitude circulation leading to SASM precipitation over the UIB region in summer season. For this, we first explored the relationship between the precipitation over UIB and mid latitude circulation. If such a relationship exists then is this robust enough to be a precursor for UIB precipitation? What are the possible mechanisms deriving this relationship between UIB precipitation and midlatitude circulation? To further elaborate our findings, we applied the regional climate model REMO over the South Asian region. Being the most intensely irrigated region in the world, it has been shown that irrigation plays a major role in modulating the weather of Indian subcontinent associated with SASM circulation (Chapter 2, (Douglas et al., 2006)). Therefore, in order to examine the effect of irrigation on UIB precipitation, we developed a simplified irrigation scheme and applied it to REMO.

This paper is designed as follows. Section 4.2 deals with the data and methodology used for the study. In Section 4.3, the effect of mid-latitude circulation over UIB precipitation is discussed. Section 4.4 comprises the simulation results of REMO model and summary and results are presented in Section 4.5.

4.2 Data and methodology

Daily averages obtained from ERA40 global fields produced by the European Centre for Medium Range Weather Forecast (ECMWF; (Uppala et al., 2005)) is the major dataset used to find the relationship between UIB precipitation and midlatitude circulation for peak summer months of July and August for 40 years from 1961 to 2000. In order to check the robustness of our results obtained from ERA40 data, we have also employed daily averages of outgoing longwave radiation (OLR) obtained through the National Oceanic and Atmospheric Administration (NOAA) satellite and daily averages of geopotential height from National Centre for Environmental Prediction (NCEP) reanalysis fields (Kalnay et al., 1996) for the time period 1979-2000.

Further the Max Planck Institute for Meteorology REgional MOdel (REMO) (Jacob, 2001; Jacob et al., 2007) has been applied over South Asian domain, forced with ERA40 data at its lateral boundaries. For this paper, we conducted two 10 year simulations at 0.5 degree resolution from 1990 to 1999, both with and without the representation of irrigation. The ability of REMO model in capturing the SASM circulation and other surface and higher level atmospheric variables has been discussed comprehensively in chapter 2 and chapter 3 of this thesis.

Moreover, for the mentioned time period of each dataset discussed above, we detrended

the daily datasets and removed the climatology to eliminate seasonal variability. Additionally we applied a 5-day running mean time filter to the daily data to eliminate synoptic variability and retain intraseasonal variability longer than 10 days. To preserve intraseasonal variability as much as possible, no other filter was applied to the data. We have mainly used correlation analysis to find the relationship between different variables. Two tailed t-test is used to check the significance of these relationships. In all the correlations plots presented in the rest of the paper, only the correlations which are significant at 99% confidence level are plotted.

In earlier studies, different areas are considered to represent the UIB (Fowler and Archer, 2006; Jain, S. K. and Agarwal, P. K. and Singh, V. P., 2007; Saeed et al., 2009b) due to different scope of those studies. For the present study we have defined the UIB as the region extending from (70° – 80° E, 30° – 36° N) as shown in the Figure 4.1. We further defined a precipitation index (PUIB) over this domain by spatially averaging the precipitation at each time step.

4.3 Mid-latitudinal influence on the precipitation over UIB

To identify the major atmospheric conditions that may precede precipitation over UIB, we have examined the correlations of 200 hPa geopotential height and OLR with PUIB. We calculated correlation between the PUIB and geopotential height at 200 hPa that is shown in Figure 4.2. Here positive values of days represent lead days with respect to PUIB at day 0. The highest correlation between PUIB and 200-hPa geopotential height occurs over the central Asian region some 3-5 days prior to the PUIB. This high pressure ridge at 200 hPa (central Asian high) is also known to effect the precipitation over central Indian monsoon region. However, as mentioned earlier, different studies show opposite relationship between this central Asian high and precipitation over this region. For example, Ramaswamy (1962) and Raman and Rao (1981) show that this central Asian high will result into a break (dry) condition over central India, whereas Kripalani et al. (1997) and Ding and Wang (2007) show that the central Asian high triggers the convection over central India leading to active (wet) conditions. However for UIB, a significant positive correlation is found between PUIB and geopotential height at 200 hPa. The high and significant correlation between PUIB and 200-hPa central Asian high has lead us to further investigate the ability of the central Asian high to be the precursor for the precipitation over UIB. For this purpose, we have defined the area-averaged 200-hPa geopotential height (GH) predictor over the central Asian domain (65° – 80° E and 35° – 45° N). Figure 4.3 shows the lead-lag correlation between GH and the PUIB for up to 15 days. The correlation between GH and PUIB reaches a maximum when GH leads PUIB by 3-4 days, suggesting the capability of the GH predictor to forecast precipitation over UIB 3-4 days prior to the occurrence of precipitation. In order to ensure the robustness of our results we have also plotted the correlations of ERA40 GH and NCEP GH with observed OLR (NOAA) over UIB. For the case of

4.3 Mid-latitude influence on the precipitation over UIB

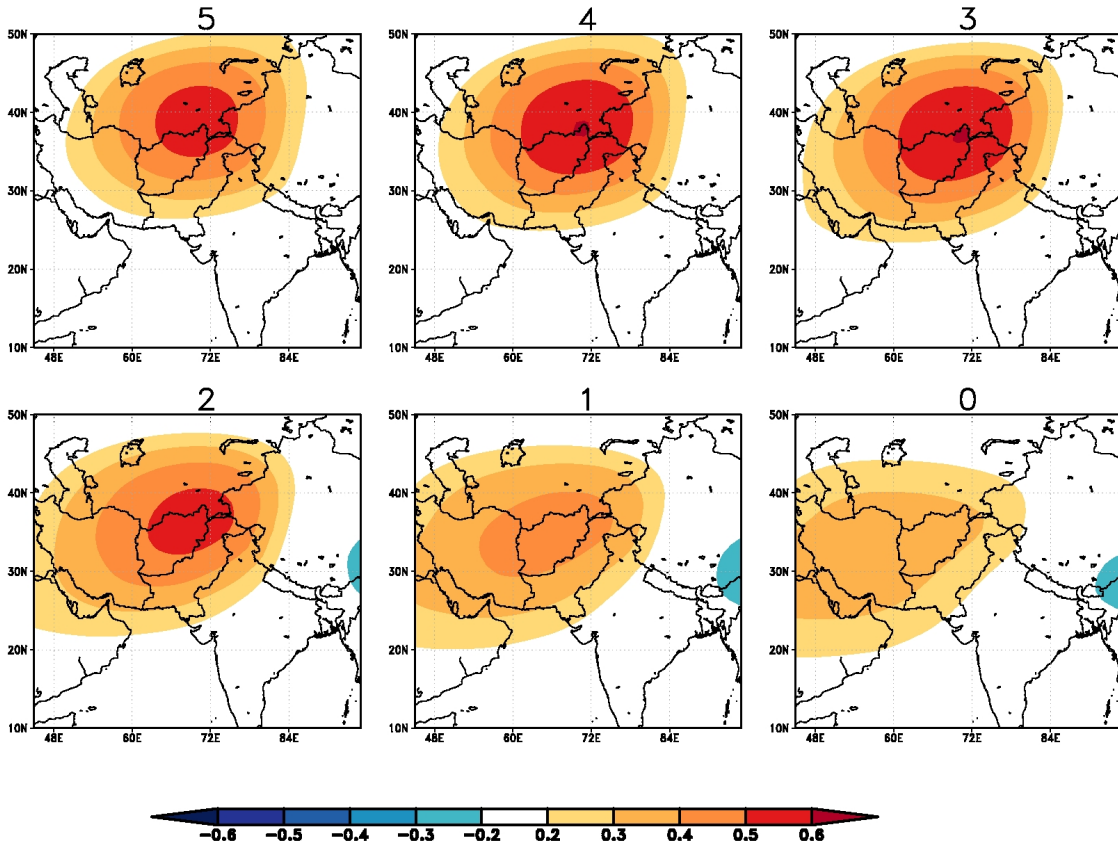


Figure 4.2: Lead-lag correlation between PUIB and 200 hPa geopotential height from ERA40 data. The positive numbers above each panel is the time in days that geopotential height leads PUIB.

ERA40 GH and observed OLR, the correlation remains as high as in the case when precipitation and GH are both used from ERA40 data. However, for the case of NCEP GH and observed OLR, the correlation slightly drops, but is reasonably high (0.47) and maintain the similar shape of the curve as in the other two cases. These results point towards the robust relationship between UIB precipitation and 200 hPa geopotential height.

In order to understand the mechanism of how the central Asian high influences the PUIB, the lead-lag correlation between PUIB and OLR is considered in Figure 4.4 which is indicating a southwest northeast pattern that starts from the 6th lead day and increases afterwards. An interesting pattern is the appearance of two highly correlated areas greater than 0.4 (one along the Arabian sea coast and other over UIB) on the 4th day prior to PUIB. Note that it is the 4th day prior to PUIB when geopotential height at 200 hPa having maximum correlation as shown in the Figure 4.2. This behavior may be attributed to the two different moisture sources over the region causing moist convection

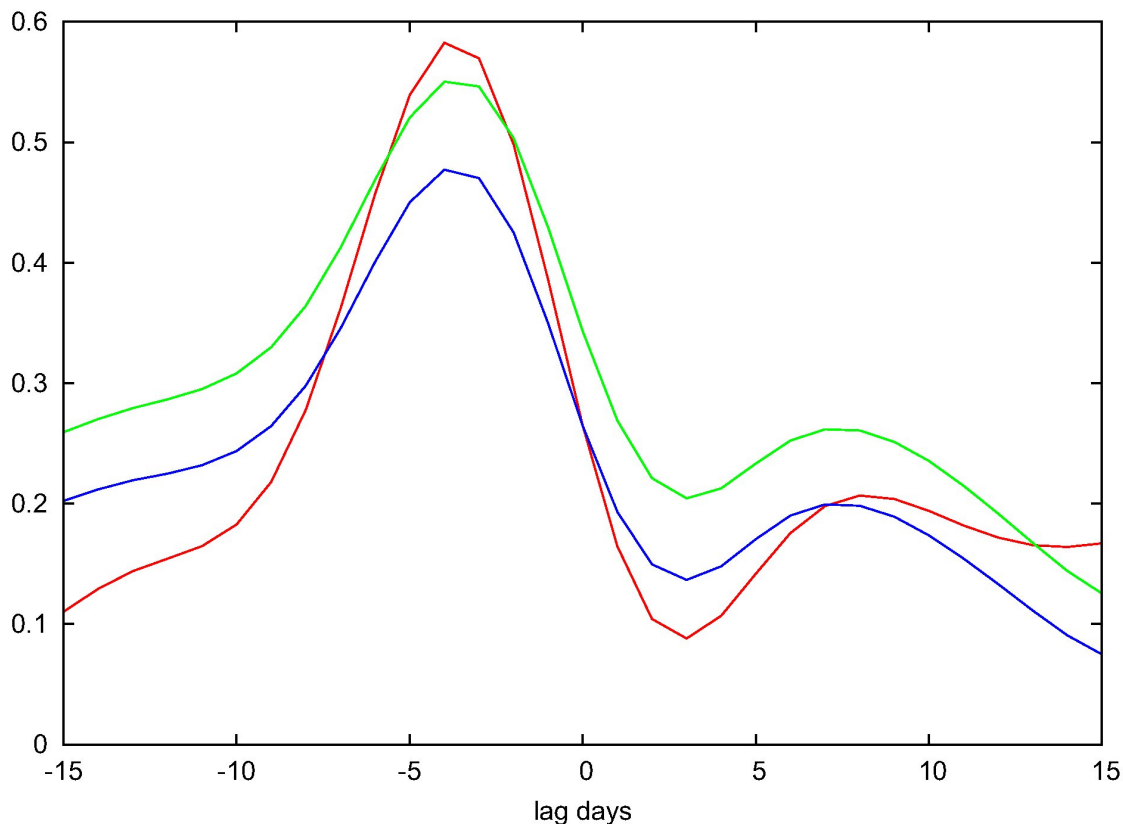


Figure 4.3: Lead-lag correlation coefficients between daily geopotential height and PUIB using ERA40 data (red curve for time period 1961-2000), between daily ERA40 geopotential height and daily OLR from NOAA (green curve for time period 1979-2000) and between daily NCEP geopotential height and daily OLR from NOAA (blue curve for time period 1979-2000). Lead-lag correlation coefficients with a lag of up to 15 days were calculated. A negative lag represents that geopotential height leads precipitation by that many days.

which will be discussed later in Section 4.3.1. To gain deeper insight into whether the southwest-northeast oriented convection pattern is independent of the central Asian high and influences the PUIB due to some other mechanism, the lead-lag correlation between GH and OLR is considered in Figure 4.5. Here, the relationship between the two of them is depicted by a reasonably high correlation. As in the case of PUIB and OLR (Figure 4.4), there are two areas of high correlations, one over UIB and the other near the southern coast. In order to find out the possible mechanism governing the relationship between GH and OLR, we calculated the correlation between GH and vertical shear of zonal winds over the region. Wind shear is calculated by U_{200} minus U_{700} , where U_{200} and U_{700} are zonal velocities at 200 hPa and 700 hPa, respectively. Figure 4.6 shows a high and significant correlation between GH and wind shear over the similar southwest-northeast oriented belt as was earlier seen in the case of GH and OLR (Figure 4.5). This

4.3 Mid-latitude influence on the precipitation over UIB

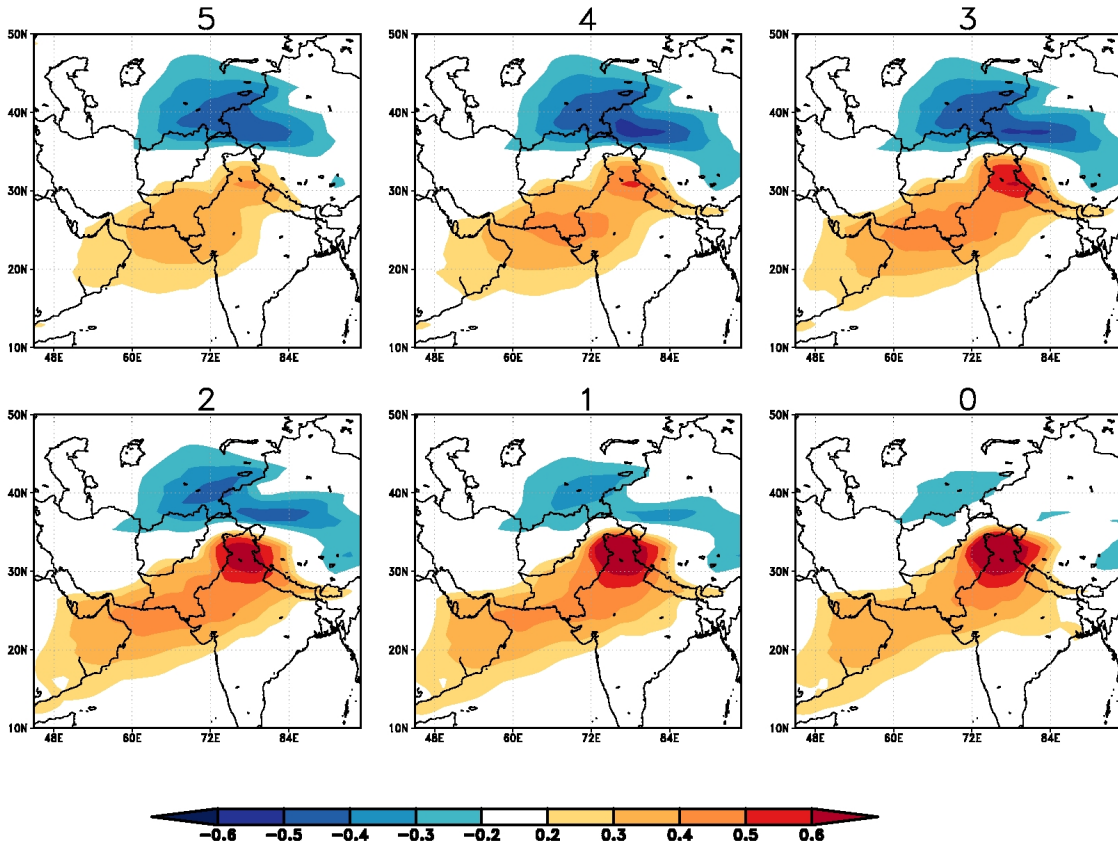


Figure 4.4: Lead-lag correlation between PUIB and OLR from ERA40 data. The positive numbers above each panel is the time in days that OLR leads PUIB.

behavior suggests that GH and UIB precipitation might be interlinked via wind shear mechanism suggested by Ding and Wang (2007). Moreover, a high negative correlation is found between GH and mean sea level pressure (MSLP; Figure 4.7) suggesting the development of low pressure predominantly over Afghanistan and Iran in response to the development of the central Asian high, similar to the one found by Saeed et al. (2010). The relationships between GH and other variables, such as wind shear and MSLP, may explain the linkage between GH and precipitation over UIB.

The possible mechanisms governing this linkage will be discussed in the following sections.

4.3.1 Proposed mechanisms influencing precipitation over UIB

With the development of the central Asian High, the circulation of the upper atmosphere changes, the characteristic Tibetan anticyclone weakens and an anomalous anticyclonic circulation gets established over the central Asian region (Saeed et al., 2010). To the south of the central Asian high, the easterly anomalies in the upper troposphere reinforce

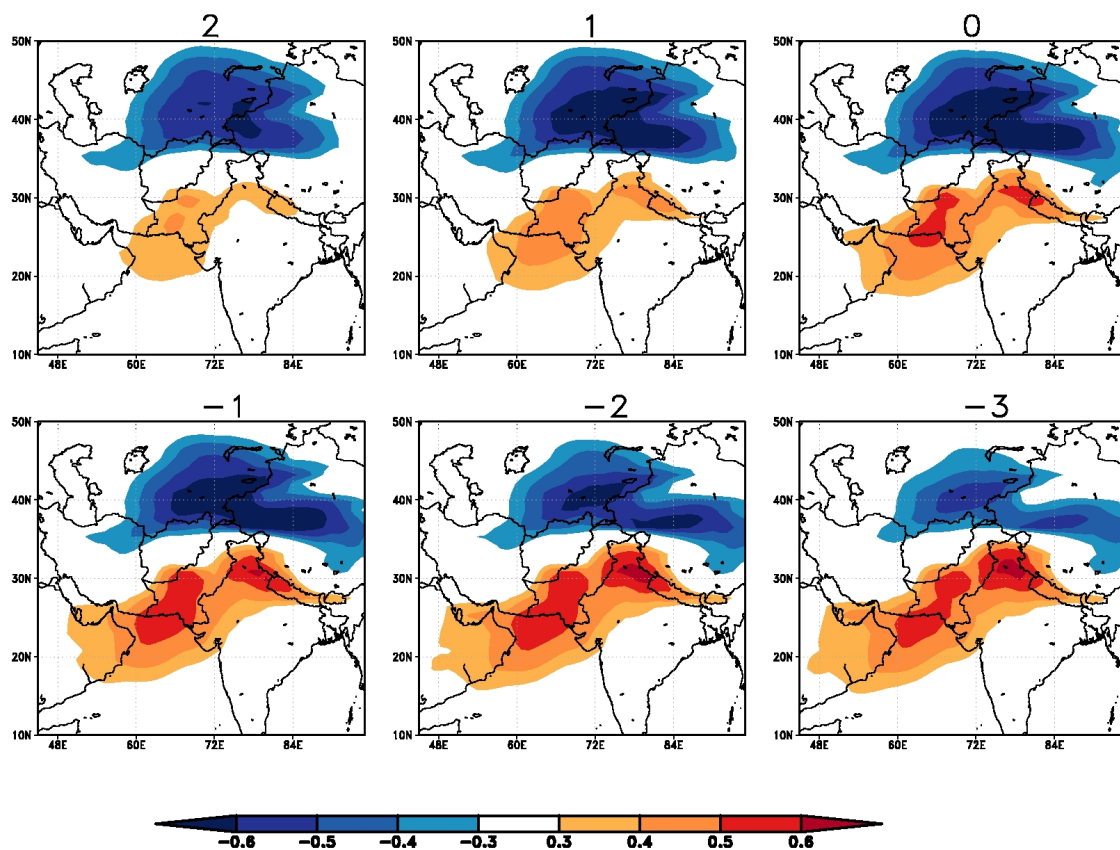


Figure 4.5: Lead-lag correlation between GH and OLR from ERA40 data. The positive/negative numbers above each panel is the time in days that OLR leads/lags GH

an easterly vertical shear in the northeast southwest direction, which has a high correlation with GH (Figure 6). This increased easterly vertical shear is responsible for the generation of an enhanced meridional heat flux that favors the conversion of mean flow available potential energy to eddy available potential energy (Ding and Wang, 2007). Therefore, it may be speculated that convection is enhanced by the increased easterly vertical shear of zonal wind over UIB.

In addition to the wind shear, Saeed et al. (2010) showed that eastward propagation of mid-latitude wave train modulate the pressure anomalies over the heat low region mainly covering Iran, Afghanistan and Pakistan. The low pressure over this region enables the moist southerly flow from the Arabian Sea to penetrate farther northward over northwestern India and Pakistan via pressure gradient mechanism. In this respect, the correlation between GH and MSLP (Figure 4.7) shows a similar relationship as found by Saeed et al. (2010).

Using REMO, it is established in chapter 2 of this thesis that large amounts of irrigated water in the summer season play a vital role in effecting the local climate of the region via

4.3 Mid-latitude influence on the precipitation over UIB

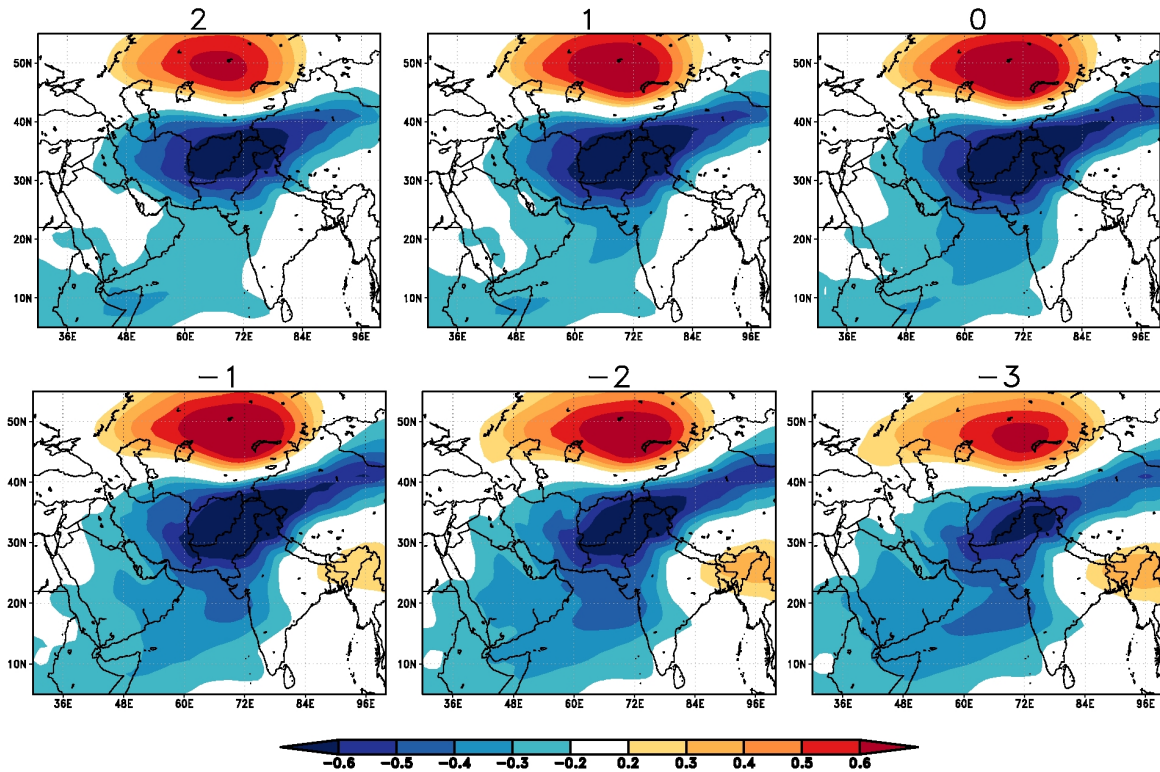


Figure 4.6: Lead-lag correlation between GH and vertical shear of zonal winds (U200 minus U700) from ERA40 data. The positive/negative numbers above each panel is the time in days that wind shear leads/lags GH.

evaporation-precipitation feedback mechanism. This feedback mechanism is also called as local recycling of moisture, because the irrigated water acts as a moisture source for convection, and results into precipitation under favorable conditions. The high value of correlation between GH and evapotranspiration in Figure 4.8 over the UIB, shows the relationship between the two.

The above-mentioned three mechanisms may be used together as an explanation of the connection between GH and PUIB. Wind shear caused by the central Asian high results into convection especially over the Arabian sea, however the dry air aloft inhibit any precipitation over the region. The resulting moisture is transported towards UIB due to pressure gradient between land and ocean which undergoes the orographic uplift due to HKH mountains in the north causing moist convection. In the meantime, the warm and dry upper level anomaly caused by central Asian high, prevents the convection by stabilizing the atmosphere, which results into a cloud free atmosphere. This causes further warming of the surface via sensible heating, and therefore resulting into the evapotranspiration of irrigated water over UIB. Therefore, in addition to the moisture advected from the south, further moisture is provided due to the evapotranspiration of irrigated water. Simultaneous occurrence of both these mechanisms cause strong moist

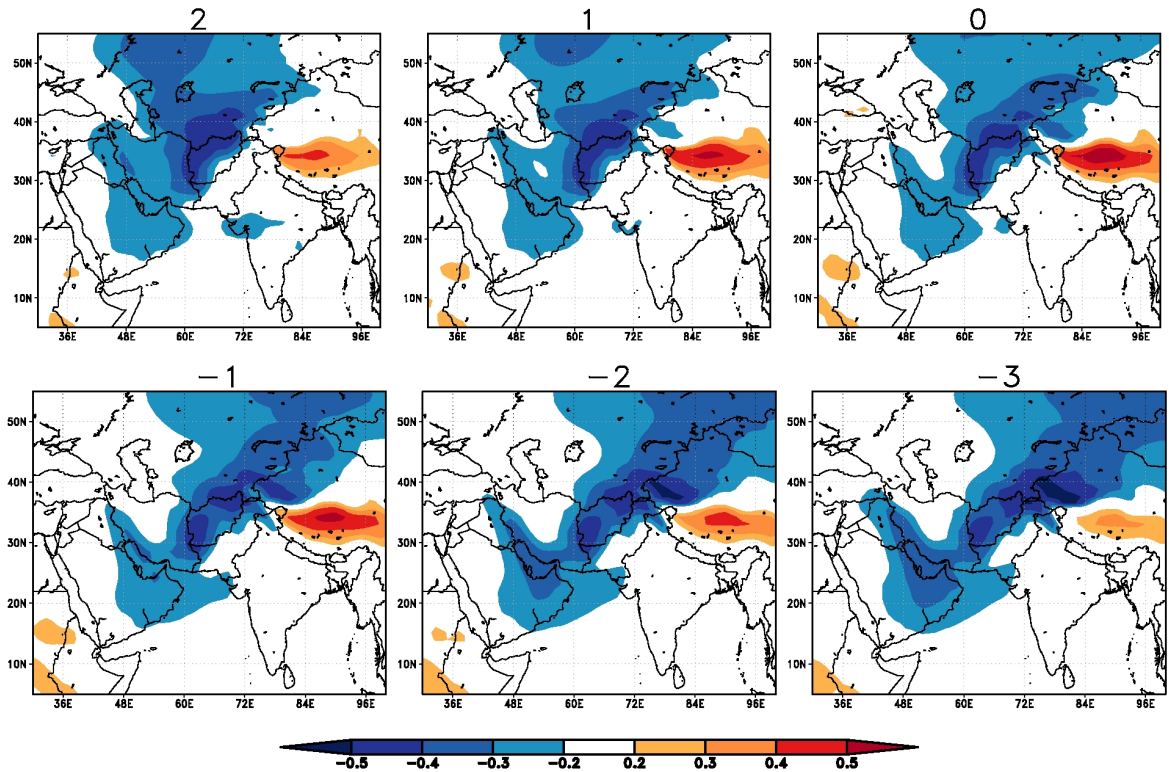


Figure 4.7: Lead-lag correlation between GH and mean sea level pressure from ERA40 data. The positive/negative numbers above each panel is the time in days that mean sea level pressure leads/lags GH.

convection, and once it becomes strong enough to overcome the stable atmosphere, it results into the initiation of precipitation.

However, it is still unclear which of the above-mentioned three mechanisms plays the most important role in connecting GH and PUIB. For this reason we conducted an experiment using the regional model REMO with the representation of irrigation as explained in the following section.

4.4 Irrigation Experiment

As mentioned above, Chapter 2 and 3 have discussed the ability of REMO in capturing the SASM circulation, its vertical structure and other surface variables such as precipitation, temperature, mean sea level pressure etc.

With the standard REMO setup, a warm bias predominantly in the area of Indus and Ganges basins came up as shown in Chapter 2. However in the sensitivity experiment with the representation of irrigation, the removal of the warm bias, along with the improved simulation of other variables had been achieved. Therefore, it was concluded that representation of irrigation is essential for the simulation of climate of the region

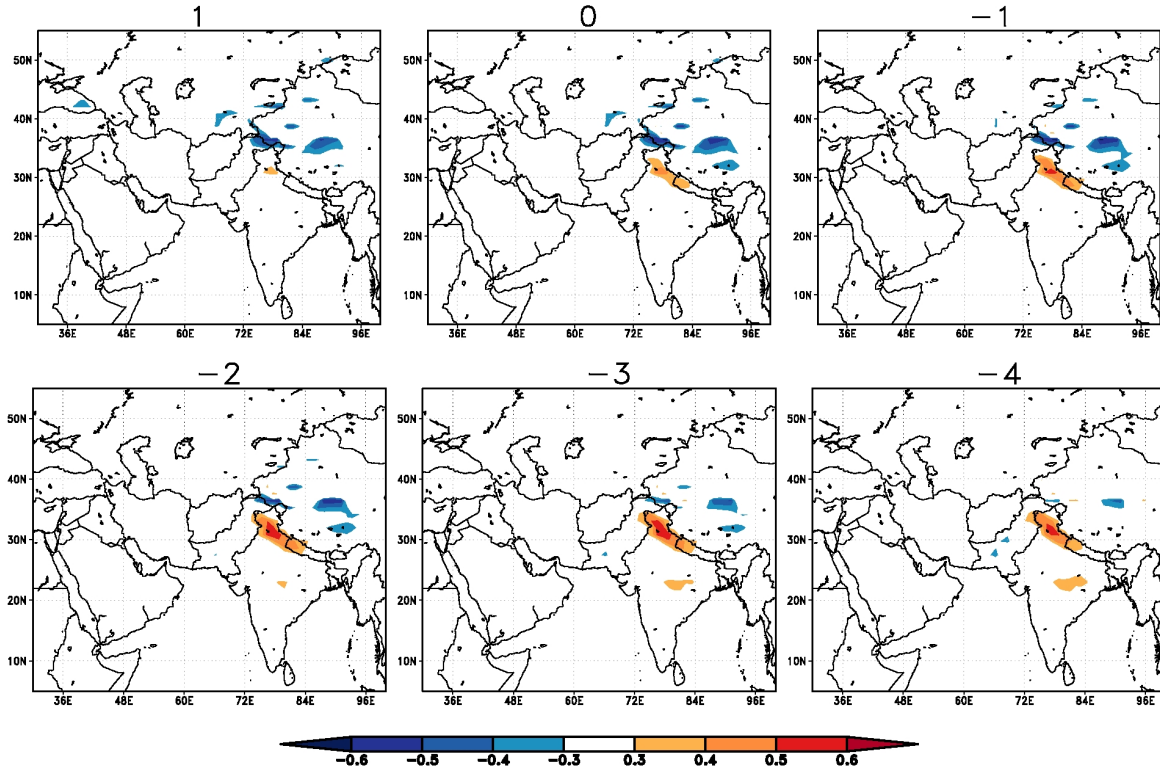


Figure 4.8: Lead-lag correlation between GH and evapotranspiration from ERA40 data. The positive/negative numbers above each panel is the time in days that evapotranspiration leads/lags GH.

in climate models. Lucas-Picher et al. (2011) intercompared 4 RCMs over SASM region and also found similar bias over the region. By referring to the study presented in chapter 2 of this thesis, they also argued that the representation of irrigation is essential for the adequate simulation of SASM. In the experiment done in chapter 2 with REMO, the irrigation was represented by a rather simplified approach. Over the irrigated fraction of a grid box soil wetness was increased to a critical value so that potential evapotranspiration could occur on each time step. However, there were two caveats in that approach: first it used a static spatial map of irrigation for the region which has strong seasonality, and second that there was an infinite availability in the amount of water to fill the irrigated part of the grid box.

In the present study, a new simplified irrigation scheme is developed whose details are given in the following section.

4.4.1 Simplified irrigation scheme

In this scheme instead of using a static irrigation map, we have used monthly irrigation map of each month as is shown in Figure 4.10 (Siebert et al., 2005). The large variability

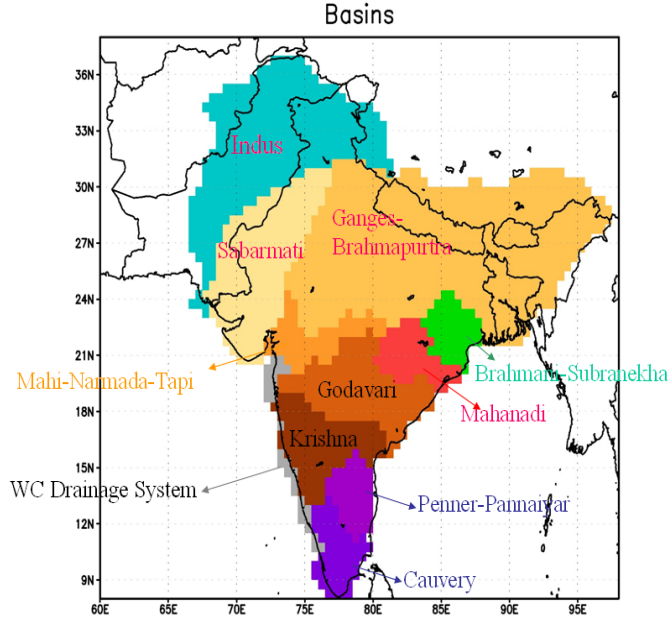


Figure 4.9: Basin masks for all the major River Basins of South Asia obtained from FAO.

in the irrigation density shows that it is more reasonable to use annual irrigation cycle instead of using a static irrigation map.

Moreover, a semi-distributed basin approach is used to implement the limitation of available water for irrigation. Figure 4.9 shows the major basins of South Asia obtained from FAO's hydroglical basins dataset for southeast Asia (www.fao.org). For each basin, we obtained the annual cycle of river runoff (mean monthly) from Center for Sustainability and the Global Environment (SAGE) river discharge database (<http://www.sage.wisc.edu/riverdata/>). We subtracted observed value of runoff from simulated value of REMO runoff for each basin at each model time step, thereby neglecting the transfer times of water within the basin:

$$RR_i - OR_i = FR_i, \text{ where } i = 1, \dots, 12 \quad (4.1)$$

where, RR is the REMO simulated runoff, OR is observed runoff and FR is the residual runoff. The residual runoff is then distributed throughout the basin depending on the irrigated grid box fraction as

$$\frac{IG_i}{IB_i} * FR_i, \text{ where } i = 1, \dots, 12 \quad (4.2)$$

where,

IG = Irrigated grid box fraction of a particular grid box

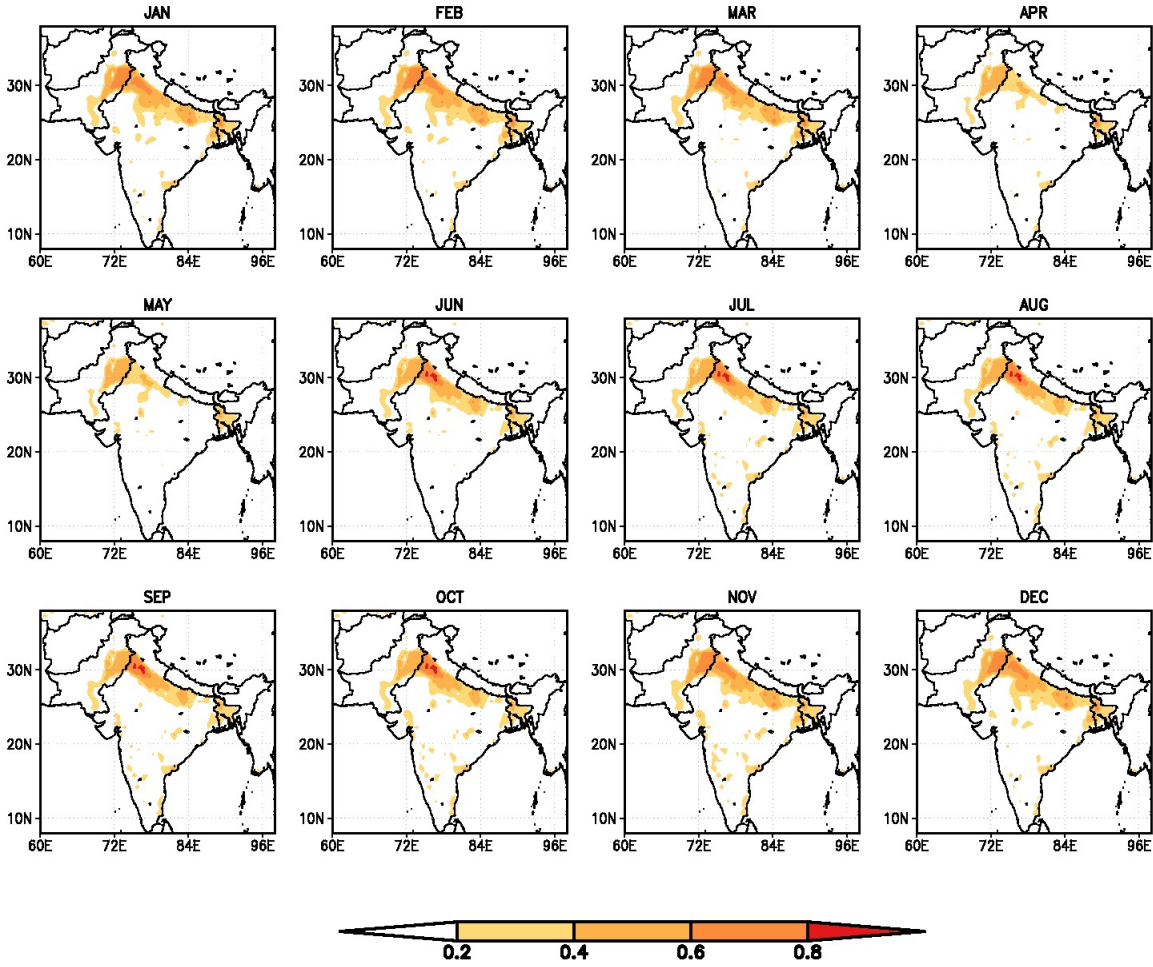


Figure 4.10: Monthly irrigation map of South Asia showing fraction of irrigated area to total area of grid box.

IB = Sum of irrigation fractions of the whole basin

This value is then added to the computed value of soil wetness in the next time step.

However, there were some basins having very little irrigated area throughout the year or very low runoff values, therefore the above mentioned approach is only applied to the Indus, Ganges-Brahmaputra, Godavari, Mahanadi, Krishna and Mahi-Narmada-Tapi basins. For the rest of the basins, equation (4.1) becomes

$$RR_i = FR_i, \text{ where } i = 1, \dots, 12 \quad (4.3)$$

For the other grid boxes inside the REMO domain but not being part of any South Asian basin (Figure 4.9), we used the same approach as was used in Chapter 2.

As mentioned earlier, we conducted two ten years simulations from 1990 to 1999 using ERA40 as lateral boundary forcings. In the first simulation we applied the standard

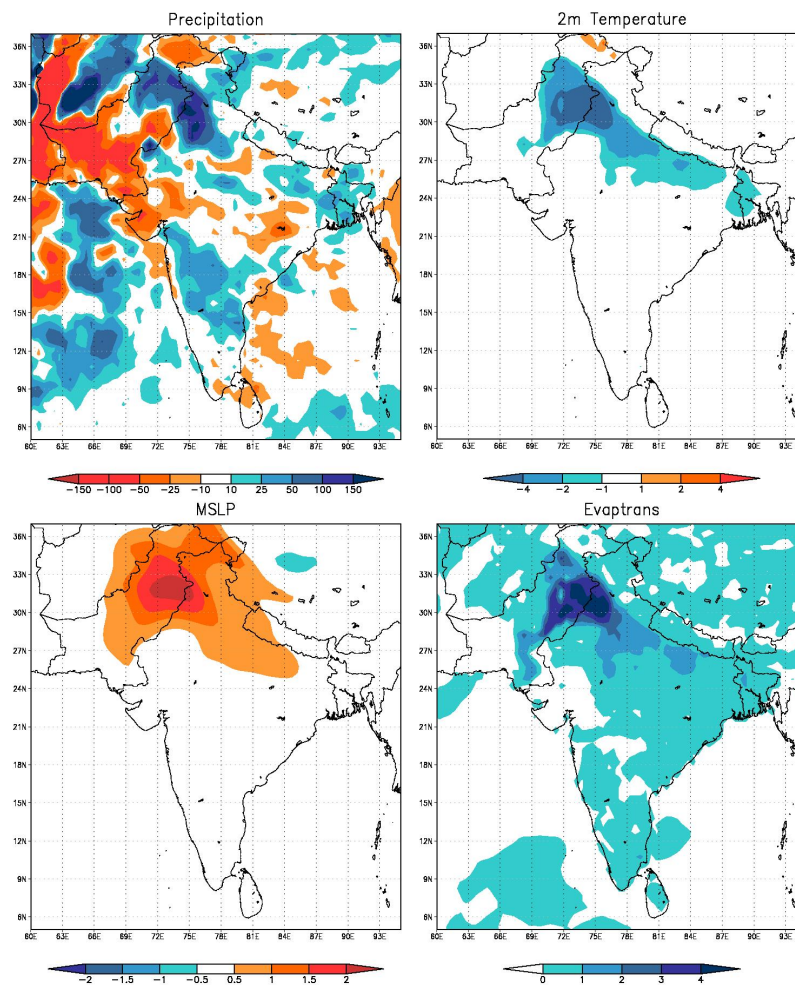


Figure 4.11: Simulated summer (JJAS) averages for 1990–1999 zoomed over the Indian subcontinent. Difference (REMO-irrigation minus REMO-baseline) of (upper left) precipitation (mm/day), (upper right) 2m temperature ($^{\circ}\text{C}$), (lower left) Mean Sea Level Pressure (hPa) and (lower right) Evapotranspiration (mm/day). Only the results significant at 95 percent from two tailed t test are shown.

REMO version without irrigation (REMO-baseline) whereas in the second simulation we applied REMO with the representation of irrigation (REMO-irrigation). The results of the two simulations are presented in the following sections.

4.4.2 Model validation and impact of irrigation

Figure 4.11 compares the changes simulated by REMO-irrigation with the REMO-baseline run for the period 1990–1999. The introduction of irrigation water has increased evapotranspiration resulting into higher amount of precipitation via evapotranspiration-precipitation feedback mechanism. This is accompanied by the removal of the temper-

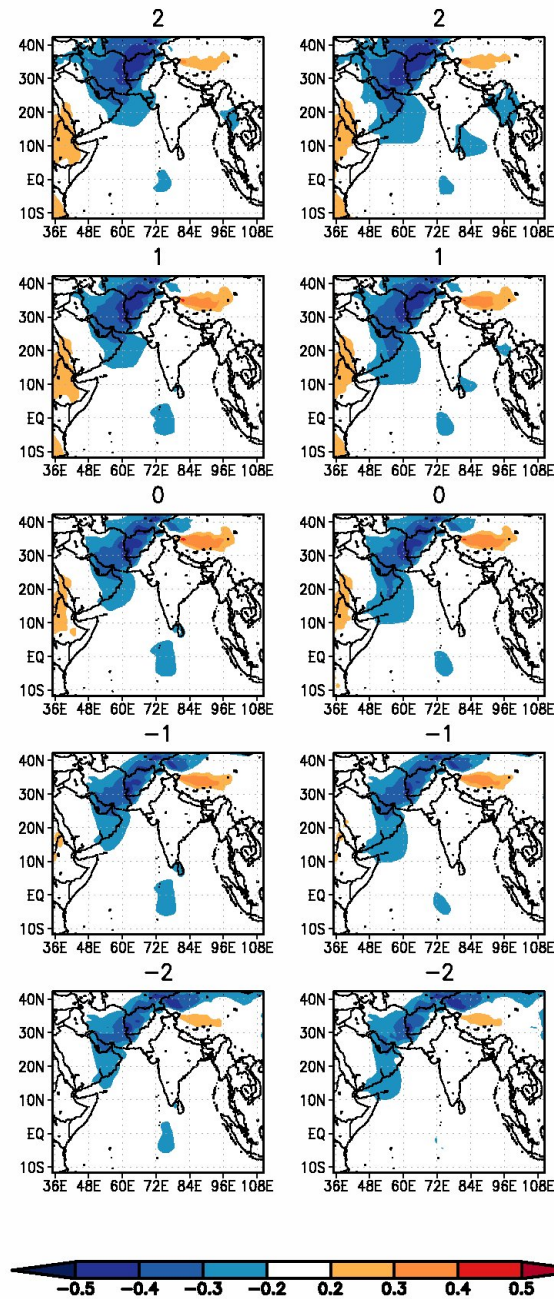


Figure 4.12: Lead-lag correlation between GH and mean sea level pressure; (left panel) REMO-irrigation and (right panel) REMO-baseline. The positive/negative numbers above each panel is the time in days that mean sea level pressure leads/lags GH.

ature bias leading to the reduced intensity of the heat low. All these results are similar to the results obtained in the second chapter. Therefore, improved irrigation scheme leads to the removal of the biases and hence, better and more realistic performance of the model.

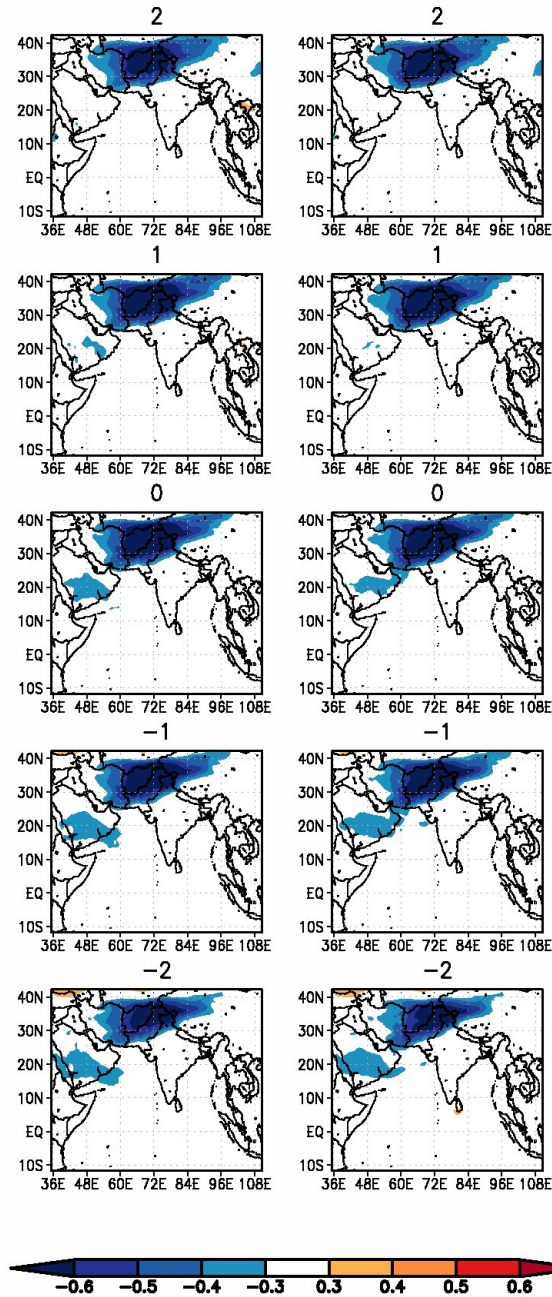


Figure 4.13: Lead-lag correlation between GH and vertical shear of zonal winds (U_{200} minus U_{700}); (left panel) REMO-irrigation and (right panel) REMO-baseline. The positive/negative numbers above each panel is the time in days that vertical wind shear leads/lags GH.

Since the northern limit of the REMO domain is at 42°N , we have modified our GH predictor to be ($65^\circ\text{--}80^\circ\text{E}$ to $35^\circ\text{--}42^\circ\text{N}$). Figure 4.12 and Figure 4.13 show the relationships for REMO-baseline and REMO-irrigation between GH and heat low and

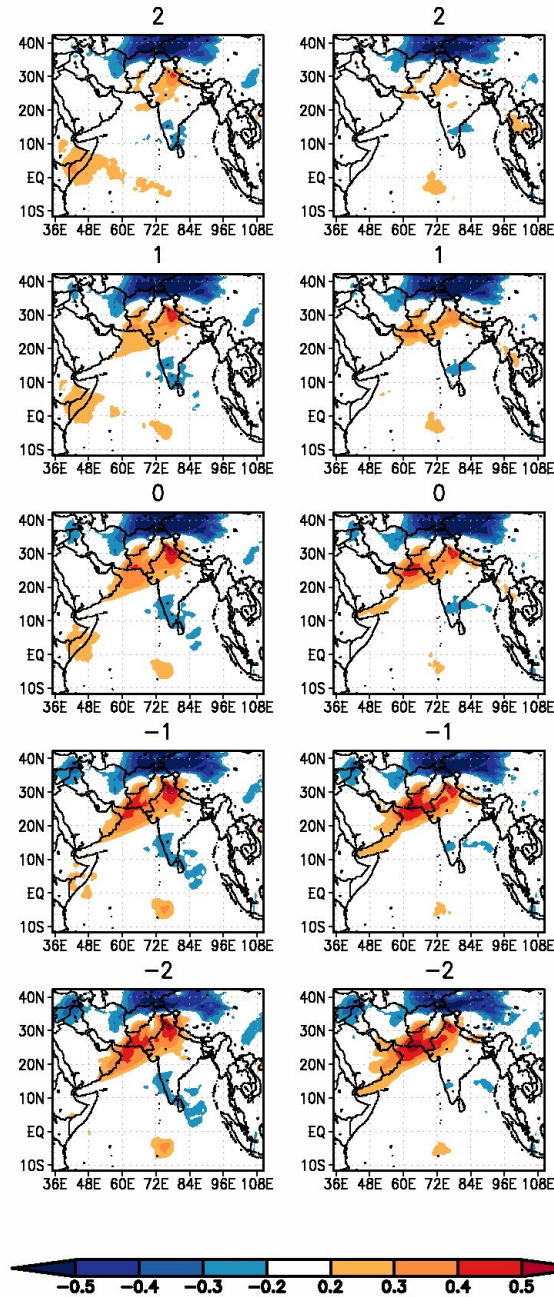


Figure 4.14: Lead-lag correlation between GH and OLR; (left panel) REMO-irrigation and (right panel) REMO-baseline. The positive/negative numbers above each panel is the time in days that OLR leads/lags GH.

between GH and wind shear, similar to the one shown in Figure 4.6 and Figure 4.7. It also depicts the ability of REMO in reproducing these relationship as was seen for the case of reanalysis data. Furthermore, two regions of convection (one along the Arabian sea coast and the other over UIB) as was seen in Figure 4.4 for ERA40 data can also be

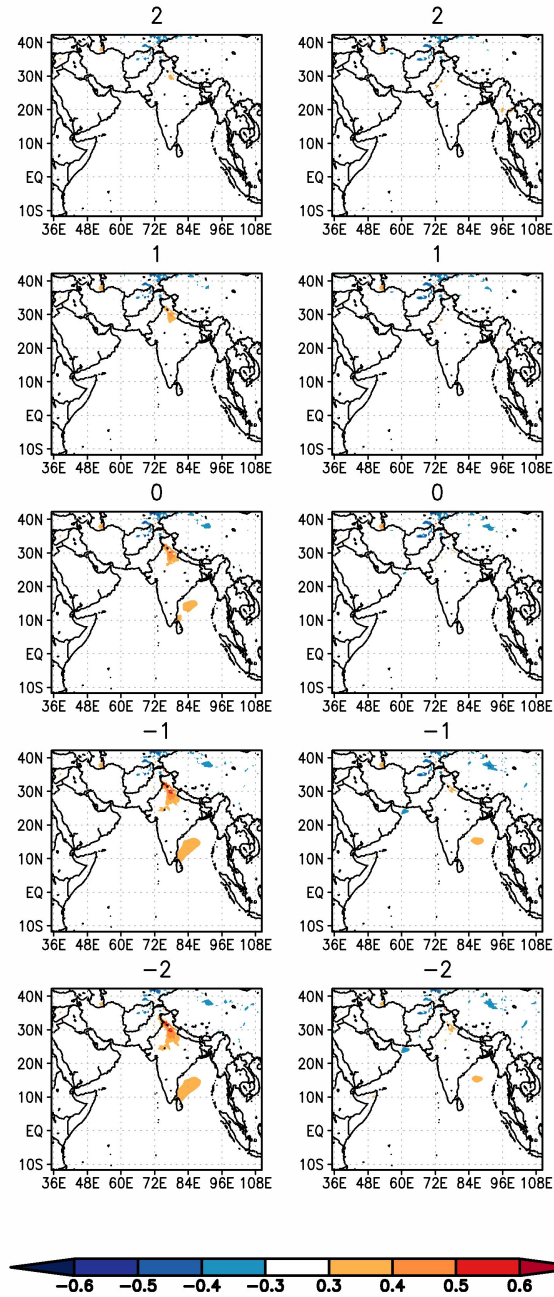


Figure 4.15: Lead-lag correlation between PUIB and evapotranspiration; (left panel) REMO-irrigation and (right panel) REMO-baseline. The positive/negative numbers above each panel is the time in days that evapotranspiration leads/lags GH.

seen in Figure 4.14 for both the REMO-baseline and REMO-irrigation.

However, for the case of REMO-irrigation run, a high correlation is found between GH and evapotranspiration over UIB (Figure 4.15), which is similar to the one found for the case of ERA40 data in Figure 4.8. Whereas, there is no such relationship found in

the case of REMO-baseline simulation. Similarly, for the case of REMO-baseline there is no relationship seen between PUIB and geopotential Height at 200 hPa, whereas for REMO-irrigation a reasonably high correlation is found (Figure 4.16). Although the correlations shown in Figure 4.16 are not as high as found for ERA40, these are still significantly higher than for REMO-baseline and at the same location as for ERA40 data (Figure 4.2).

From these results it can be concluded that water used for irrigation plays a significant role in effecting the precipitation over UIB region. Although the land sea thermal contrast as suggested by Saeed et al. (2010) is also an important factor for advection of moisture to UIB (as indicated by two convection zones in Figure 4.14 for REMO-baseline), it does not account for the total precipitation over UIB. The higher correlation in Figure 4.16 for the REMO-irrigation simulation shows that irrigation water plays a crucial role for the provision of sufficient moisture in order to overcome the preexisting stable atmosphere, and therefore the initiation of precipitation.

4.5 Summary and Discussion

In the present study, the attention is focussed over Upper Indus Basin (UIB), which is very crucial but neglected area for atmospheric research over South Asia. Using ERA40 data, it is found that for the peak summer month of July and August there is a reasonable correlation between PUIB (precipitation averaged over UIB domain) and geopotential height at 200 hPa. Based on this relationship, a 200-hPa geopotential height index GH has been defined and it is showed that GH has the ability to serve as precursor for precipitation over UIB. For the robustness of this result, a similar relationship between GH and PUIB has been found using observed OLR and NCEP reanalysis data.

After establishing the link between GH and PUIB, the attention is paid on the mechanism by which GH effects precipitation over UIB. Two regions of higher correlation between GH and OLR are identified, one over the coastal region and another over the UIB. It is argued that the upper tropospheric winds on the southern side of the central Asian high cause the convection near the ocean via wind shear mechanism but does not result into precipitation due to presence of dry and warm air aloft. The moisture present in the atmosphere is then transported towards the UIB because of the pressure gradient between land and ocean. Further moisture is supplied due to the evapotranspiration of irrigated water caused by the sensible heating due to cloud free conditions associated with central Asian high. Once the moisture from evapotranspiration, along with the moisture advection from the Arabian sea becomes sufficient to overcome the stable atmospheric conditions associated with the central Asian high, precipitation is initiated over UIB.

In order to further explore the linkage between GH and PUIB in the light of above mentioned mechanisms, an irrigation experiment has been conducted using the regional climate model REMO. The improved representation of irrigation in REMO results into the removal of biases and better simulation of other surface variables, similar to those shown in second chapter of this thesis. It is further shown that both model versions,

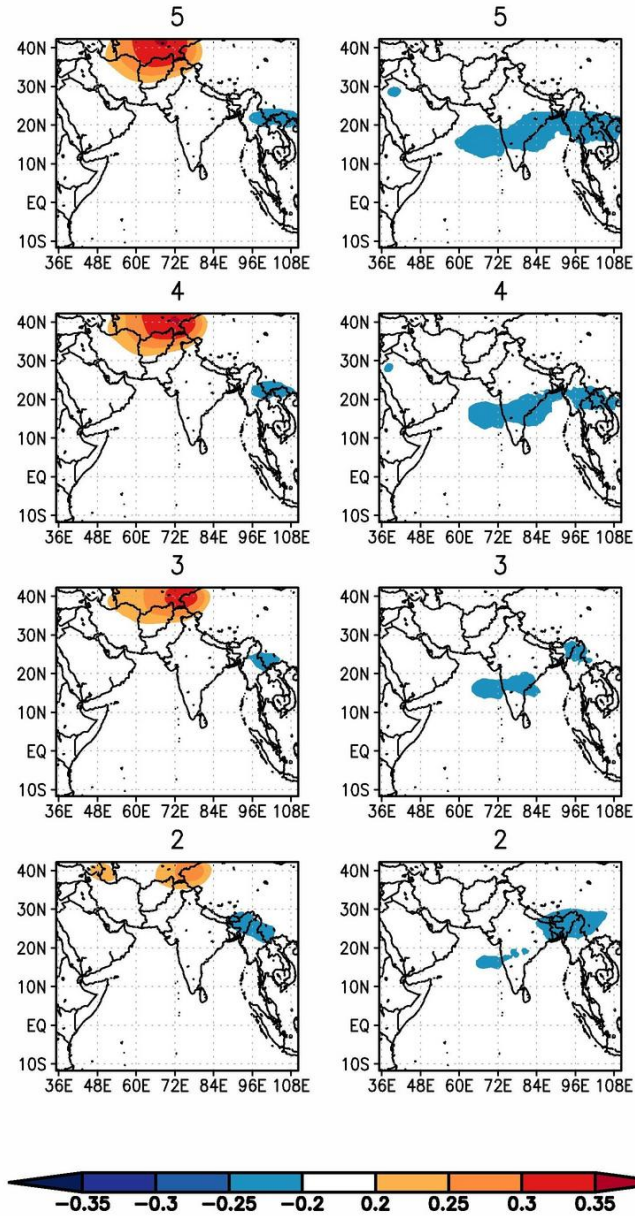


Figure 4.16: Lead-lag correlation between PUIB and 200 hPa geopotential height; (left panel) REMO-irrigation and (right panel) REMO-baseline. The positive/negative numbers above each panel is the time in days that 200 hPa geopotential height leads/lags PUIB.

REMO-baseline and REMO-irrigation, show similar significant correlation between GH and wind shear and between GH and Heat low index. Two regions of convection, one over UIB and the other over coastal region in the south, are found for both REMO-

irrigation and REMO-baseline versions which are similar to those shown by ERA40 data. However REMO-baseline version does not show any correlation between GH and evapotranspiration as well as between PUIB and geopotential height at 200 hPa, contrary to that of ERA40 and REMO-irrigation which show reasonably high correlations between them.

From these results it is concluded that during summer months of July and August, although differential heating mechanism due to central Asian high as suggested by Saeed et al. (2010), also cause advection of moisture from Arabian Sea towards UIB, however it is not sufficient for the precipitation over UIB. The necessary moisture is supplied by the evapotranspiration of the irrigated water, causing convection and hence resulting into precipitation which is further supported by the complex topography of the region.

Considering the large impact of irrigation on UIB precipitation, one can assume that under global warming the changes in the timings of water inflows would shift towards earlier months, hence causing changes in cropping patterns and subsequently irrigation. Therefore, the present study also calls for the need of representation of irrigation in climate models for analyzing the effect of climate change over the region.

5 Conclusions and Outlook

5.1 Summary

In this thesis the regional climate model REMO is applied over the south Asian region in order to study the impact of irrigation on the climate of the region. Within this work, all the simulations were carried out at 0.5° resolution over the South Asian domain, forced with ERA40 reanalysis data at the lateral boundaries.

The initial application of REMO over South Asian domain showed reasonably good agreement with observations and reanalysis data in capturing different features such as wide range of 2m temperature, the location of heat low, the lower tropospheric winds and precipitation patterns. However, a warm and dry bias appeared over the western India and Pakistan region. This bias was occurring over the heat low region, which is known to strongly affect the movement of depressions especially from the bay of Bengal. However, the occurrence of this bias over the most intensely irrigated region of the world (Indus and Ganges basin) pointed towards the lack of representation of irrigation in REMO. Therefore in order to address this bias, a sensitivity experiment of irrigation in REMO was conducted. With the representation of irrigation a more realistic simulation of SASM was achieved, causing the removal of the warm bias and hence, resulting into a better representation of a less intensified heat low. The addition of irrigation water also led to the removal of the dry bias by local recycling of water via the evaporation-precipitation feedback mechanism. Furthermore, a more realistic representation of the heat low made the conditions favorable for the depressions from bay of Bengal to intrude westward deep into the land areas.

By then it was established that irrigation plays a major role in effecting the SASM circulation and associated rainfall, however the performance of REMO over the SASM region was considered rather briefly and it was restricted to surface variables such as temperature, mean sea level pressure, precipitation and low-level winds. Considering the complexities and deep vertical structure associated with the SASM system, there was a need to evaluate these results in much more detail. For this purpose a comprehensive framework was proposed for the evaluation of SASM in a climate model. This framework includes different indices related to the movement of the inter tropical convergence zone (ITCZ), the onset, duration, and vertical structure of SASM. Based on this criteria, the performance of REMO was evaluated against observations as well as reanalysis data. REMO demonstrated good skill in fulfilling the criteria presented in the framework.

Finally the attention was focused on the Indus basin, precisely upper Indus basin (UIB), which is a very crucial but previously neglected area for atmospheric research over South Asia. Using reanalysis and satellite datasets, a robust relationship between

summer precipitation over UIB and mid-latitude circulation was found. It was also discussed that the central Asian high at 200 hPa, which is associated with mid-latitude circulation, has the ability to be a precursor for UIB precipitation. In order to highlight the role of irrigation in explaining the link between the central Asian high and precipitation over UIB, a simplified irrigation scheme was developed and implemented into REMO. Here, the REMO simulation with the simplified irrigation scheme showed a significant positive correlation between central Asian high and precipitation over UIB, contrary to REMO simulation without the irrigation scheme which showed only a weak relationship between the two. Therefore, it was concluded that although moisture is also advected from the Arabian sea over the UIB via the pressure gradient mechanism, the decisive role is played by the irrigated water in providing necessary moisture for the precipitation over UIB.

In the introductory chapter of this thesis several research questions had been raised. Based on the analyses conducted within this work the major findings with respect to these research focal points are listed as follows:

i) In chapter 2, the ability of REMO in capturing the surface variables such as 2m temperature, mean sea level pressure, low level winds and precipitation over SASM region was shown. REMO did a satisfactory job in capturing the low-level SASM behavior. Moreover, in chapter 3 a new framework for the evaluation of climate models for its application over SASM region was proposed. This framework is then applied to REMO and it was noticed that within this new framework, REMO performed well in capturing the deep vertical structure defined by different indices. Hence, it is concluded that along with the surface variables, REMO has the ability to simulate the complex vertical structure associated with SASM.

ii) Although REMO performed reasonably well over SASM region, a prominent bias was noticed in the overestimation of 2m temperature leading to the unrealistic intensification of the heat low. Since South Asia is the most intensely irrigated region in the world, the non-representation of irrigation in REMO was identified as the main cause leading to this bias.

iii) The above mentioned bias is not limited to REMO only. A recent study (Lucas-Picher et al., 2011) found the similar bias in other regional climate models as well. While referring to the study presented in Chapter 2, they concluded that representation of irrigation was the main cause leading to this bias. In REMO, the sensitivity study with irrigation showed the removal of this temperature bias. It was noticed that irrigation does not only have a local effect, but also influences the climate of whole South Asia.

iv) In chapter 4, the relationship between mid-latitude circulation and precipitation over UIB was identified using reanalysis and observational datasets. It was argued that this relationship has the potential to serve as a precursor for UIB precipitation. With the development of a simplified irrigation scheme and its application to REMO, it was shown that irrigation plays a significant role in strengthening the relationship between mid-latitude circulation and UIB precipitation.

5.2 Outlook

The presented studies are amongst the first to use a climate model for assessing the role of irrigation in impacting the climate of the South Asian region. These studies raise many other questions regarding the effects of irrigation on future climate of the region.

Chapter 2 and 3 showed that the REMO model is well suited for conducting climate change simulations over the South Asia region. Consequently for the purpose of studying the potential impacts of climate change over the region, transient climate change simulations were conducted. The results of these simulations are being analyzed for a cooperative study under the European Union project Water and Global Change (WATCH).

Considering the huge impact of irrigation on regional climate, the present study calls for the need of development of a more sophisticated irrigation scheme to serve as an integral part of earth system models. For this purpose, a more dedicated effort has to be made to collect irrigation related observational data (e.g. spatial coverage of irrigated land, canal diversions, availability of water at farm gate etc.) from countries around the globe. Furthermore, other human modifications to the hydrological cycle, such as reservoirs, link canals and other diversions should be incorporated in the next generation of climate models to elucidate the feedbacks between human water use and climate.

It is also important to take account of how the changing melt water regime of Himalayan-Karakoram-Hindukush ranges will affect the irrigation patterns. For example, 80% of the Indus basin river flow is attributed to the melt of snow and glaciers. Considering the large impact of irrigation on SASM behaviour, one can assume that under global warming the changes in the timings of water inflows would shift towards earlier months, hence causing changes in cropping patterns and subsequently irrigation.

It will be vital to answer that considering the substantial role of irrigation on the region, how the climate of South Asia will respond to the global warming. It has been hypothesized that irrigation-related cooling in certain regions of the world has "masked" the global warming regionally Puma and Cook (2010). However there is no such study for South Asia. There is a plan to conduct a study under the WATCH project in the near future, where more than one RCM will be used to analyse the effect of irrigation in future climate for the region.

6 Acknowledgements

First and the foremost, I want to express my deepest gratitude to my supervisor Stefan Hagemann, for his invaluable favors and kindness. He guided my work with patience, enthusiasm and a great amount of tolerance. I appreciate his help in providing me with the money for attending many informative and helpful meetings and conferences during my PhD.

My most profound thanks go to Daniela Jacob, for partially supervising my research work and for the various bits of knowledge and wisdom which she impart to me during various stages of this work. I always could rely on her remarkable ability to quickly distill any problem to its essence.

I extend my gratitude to Martin Claussen, as my panel chair, who provided some very clear and fruitful comments during the panel meetings.

Financial support of the Higher Education Commission of Pakistan for conducting this PhD work under the project “Overseas Scholarship for PhD in Selected fields” is greatly acknowledged.

I wish to thank my worthy group-mates from the Terrestrial Hydrology Group and the Regional Modelling Group at the Max Planck Institute for Meteorology for such a friendly, cooperative and inspiring atmosphere to enjoy my work.

A very big thank you goes to my office mates during the last years: Tanja Blome, Cui Chen, Andreas Haensler and Tobias Stacke, for their support. I am immensely grateful to you for making this time such a pleasant and memorable one, with many fruitful discussions on various topics. Thanks are due to Sajjad Saeed for being such a terrific fellow during these years. I also highly value advices from my former colleague Jan Haerter.

I can never thank enough my family for their support. Even then, I wish to record my deepest obligations to my parents who have always supported me unconditionally and selflessly. A great thank you to my friends here in Germany for making me feel at home. Last but not least, I would always be indebted to the love and care of my wife Mariam - thanks a lot for making it so special.

6 Acknowledgements

Bibliography

- Annamalai, H., Slingo, J. M., Sperber, K. R., Hodges, K., 1999. The mean evolution and variability of the Asian summer monsoon: Comparison of ECMWF and NCEP-NCAR reanalyses. *Mon. Wea. Rev.* 127 (6, Part 2), 1157–1186.
- Archer, D. R., Forsythe, N., Fowler, H. J., Shah, S. M., 2010. Sustainability of water resources management in the Indus Basin under changing climatic and socio economic conditions. *Hydrol. Earth Syst., Sci.* 14 (8), 1669–1680.
- Ashfaq, M., Shi, Y., Tung, W., Trapp, R. J., Gao, X., Pal, J. S., Diffenbaugh, N. S., 2009. Suppression of south Asian summer monsoon precipitation in the 21st century. *Geophys. Res. Lett.* 36 (1), DOI: 10.1029/2008GL036500.
- Barker, R., Molle, F., 2004. Evolution of irrigation in South and Southeast Asia. Colombo, Sri Lanka: Comprehensive Assessment Research Report 5. ISBN: 9290905603.
- Bhaskar Rao, D. V., Ashok, K., Yamagata, T., 2004. A numerical simulation study of the indian summer monsoon of 1994 using near mm5. *J. Meteorol. Soc. Jpn.* 82 (6), 1755–1775.
- Bhaskaran, B., Jones, R. G., Murphy, J. M., Noguer, M., 1996. Simulations of the Indian summer monsoon using a nested regional climate model: Domain size experiments. *Clim. Dyn.* 12 (9), 573–587.
- Boucher, O., Myhre, G., Myhre, A., 2004. Direct human influence of irrigation on atmospheric water vapour and climate. *Clim. Dyn.* 22 (6-7), 597–603.
- Branstator, G., 2002. Circumglobal teleconnections, the jet stream waveguide, and the North Atlantic oscillation. *J. Clim.* 15 (14), 1893–1910.
- Cadet, D., 1979. Meteorology of the Indian summer monsoon. *Nature* 279, 761–767.
- Cotton, W. R., Pielke, R. A., 2007. *Human Impacts on Weather and Climate*. Cambridge University Press, U.K, ISBN: 0521840864.
- Dash, S. K., Shekhar, M. S., Singh, G. P., 2006. Simulation of Indian summer monsoon circulation and rainfall using RegCM3. *Theo. App. Clim.* 86 (1-4), 161–172.
- Davies, H., 1976. Lateral boundary formulation for multilevel prediction models. *Quart. J. Royal Meteorol. Soc.* 102 (432), 405–418.

Bibliography

- de Rosnay, P., Polcher, J., Laval, K., Sabre, M., 2003. Integrated parameterization of irrigation in the land surface model ORCHIDEE. Validation over Indian Peninsula. *Geophys. Res. Lett.* 30 (19), HLS2-1-4.
- Ding, Q., Wang, B., 2007. Intraseasonal teleconnection between the summer Eurasian wave train and the Indian monsoon. *J. Clim.* 20 (15), 3751-3767.
- Ding, Q. H., Wang, B., 2005. Circunglobal teleconnection in the Northern Hemisphere summer. *J. Clim.* 18 (17), 3483-3505.
- Dobler, A., Ahrens, B., 2010. Analysis of the Indian summer monsoon system in the regional climate model COSMO-CLM. *J. Geo. Res.-Atm.* 115, DOI: 10.1029/2009JD013497.
- Douglas, E. M., Beltran-Przekurat, A., Niyogi, D., Pielke, Sr., R. A., Vorosmarty, C. J., 2009. The impact of agricultural intensification and irrigation on land-atmosphere interactions and Indian monsoon precipitation - A mesoscale modeling perspective. *Glob. Planet. Chg.* 67 (1-2), 117-128.
- Douglas, E. M., Niyogi, D., Froking, S., Yeluripati, J. B., Pielke, Sr., R. A., Niyogi, N., Voeroesmarty, C. J., Mohanty, U. C., 2006. Changes in moisture and energy fluxes due to agricultural land use and irrigation in the Indian Monsoon Belt. *Geophys. Res. Lett.* 33 (14), DOI: 10.1029/2006GL026550.
- Fowler, H. J., Archer, D. R., 2006. Conflicting signals of climatic change in the Upper Indus Basin. *J. Clim.* 19 (17), 4276-4293.
- Gadgil, S., Sajani, S., 1998. Monsoon precipitation in the AMIP runs. *Clim. Dyn.* 14 (9), 659-689.
- Giorgi, F., 2006. Regional climate modeling: Status and perspectives. *J. de Phys.* 4. 139, 101-118.
- Goswami, B. N., 1998. Interannual variations of Indian summer monsoon in a GCM: External conditions versus internal feedbacks. *J. Clim.* 11 (4), 501-522.
- Goswami, B. N., Krishnamurthy, V., Annamalai, H., 1999. A broad-scale circulation index for the interannual variability of the Indian summer monsoon. *Quart. J. Royal Meteorol. Soc.* 125 (554, Part B), 611-633.
- Goswami, B. N., Mohan, R. S. A., 2001. Intraseasonal oscillations and interannual variability of the Indian summer monsoon. *J. Clim.* 14 (6), 1180-1198.
- Goswami, B. N., Xavier, P. K., 2005. ENSO control on the south Asian monsoon through the length of the rainy season. *Geophys. Res. Lett.* 32 (18).
- Haensler, A., Hagemann, S., Jacob, D., 2010. Dynamical downscaling of ERA40 reanalysis data over southern Africa: added value in the representation of seasonal rainfall characteristics. *Int. J. Climatol* DOI: 10.1002/joc.2242.

- Hagemann, S., 2002. An improved land surface parameter dataset for global and regional climate models. Report 336, Max-Planck-Inst. Meteorol., Hamburg, Germany.
- Hagemann, S., Botzet, M., Dumenil, L., Machenhauer, B., 1999. Derivation of global GCM boundary conditions from 1 km land use satellite data. Report 289, Max-Planck-Inst. Meteorol., Hamburg, Germany.
- Hagemann, S., Gates, L. D., 2003. Improving a subgrid runoff parameterization scheme for climate models by the use of high resolution data derived from satellite observations. *Clim. Dyn.* 21 (3-4), 349–359.
- Halpern, D., Woiceshyn, P. M., 1999. Onset of the Somali Jet in the Arabian Sea during June 1997. *J. Geophys. Res.-Ocn.* 104 (C8), 18041–18046.
- He, H. Y., Sui, C. H., Jian, M. Q., Wen, Z. P., Lan, G. D., 2003. The evolution of tropospheric temperature field and its relationship with the onset of Asian summer monsoon. *J. Meteorol. Soc. Jpn.* 81 (5), 1201–1223.
- Hoskins, B. J. and Wang, B., 2005. Large-scale atmospheric dynamics. In: Wang B (ed) *The Asian monsoon*. Springer-Praxis, the Netherlands, pp. 357–415.
- Jacob, D., 2001. A note to the simulation of the annual and inter-annual variability of the water budget over the Baltic Sea drainage basin. *Meteorol. Atmos. Phys.* 77, 61–73.
- Jacob, D., 2008. *Klimaauswirkungen und Anpassung in Deutschland—Phase 1: Erstellung regionaler Klimaszenarien für Deutschland*. Abschlussbericht zum UFOPLAN-Vorhaben 204, 41–31.
- Jacob, D., Barring, L., Christensen, O. B., Christensen, J. H., de Castro, M., Deque, M., Giorgi, F., Hagemann, S., Lenderink, G., Rockel, B., Sanchez, E., Schaer, C., Seneviratne, S. I., Somot, S., van Ulden, A., van den Hurk, B., 2007. An inter-comparison of regional climate models for Europe: model performance in present-day climate. *Clim. Chg.* 81 (Suppl. 1), 31–52.
- Jain, S. K. and Agarwal, P. K. and Singh, V. P., 2007. *Hydrology and water resources of India*. Springer, the Netherlands, ISBN: 9781402051791(H).
- Jayaraman, K. S., 2005. Rival monsoon forecasts banned. *Nature* 436, 161.
- Ji, Y. M., Vernekar, A. D., 1997. Simulation of the Asian summer monsoons of 1987 and 1988 with a regional model nested in a global GCM. *J. Clim.* 10 (8), 1965–1979.
- Kalnay, E., Kanamitsu, M., Kistler, R., Collins, W., Deaven, D., Gandin, L., Iredell, M., Saha, S., White, G., Woollen, J., Zhu, Y., Chelliah, M., Ebisuzaki, W., Higgins, W., Janowiak, J., Mo, K. C., Ropelewski, C., Wang, J., Leetmaa, A., Reynolds, R., Jenne, R., Joseph, D., 1996. The NCEP/NCAR 40-year reanalysis project. *Bull. Amr. Meteorol. Soc.* 77 (3), 437–471.

Bibliography

- Karim, A., Veizer, J., 2002. Water balance of the Indus River Basin and moisture source in the Karakoram and western Himalaya: Implications from hydrogen and oxygen isotopes in river water. *J. Geophys. Res.* 107 (D18), DOI: 10.1029/2000JD000253.
- Katz, R. W., 2002. Sir Gilbert Walker and a connection between El Nino and statistics. *Stats. Sci.* 17 (1), 97–112.
- Khan, S., Rana, T., Gabriel, H. F., Ullah, M. K., 2008. Hydrogeologic assessment of escalating groundwater exploitation in the Indus Basin, Pakistan. *Hydrogeol. J.* 16 (8), 1635–1654.
- Kripalani, R. H., Kulkarni, A., Singh, S. V., 1997. Association of the Indian summer monsoon with the Northern Hemisphere mid-latitude circulation. *Int. J. Climatol.* 17 (10), 1055–1067.
- Kripalani, R. H., Oh, J. H., Kulkarni, A., Sabade, S. S., Chaudhari, H. S., 2007. South Asian summer monsoon precipitation variability: Coupled climate model simulations and projections under IPCC AR4. *Theo. App. Climatol.* 90 (3-4), 133–159.
- Krishnamurthy, V., Goswami, B. N., 2000. Indian monsoon-ENSO relationship on interdecadal timescale. *J. Clim.* 13 (3), 579–595.
- Kueppers, L. M., Snyder, M. A., Sloan, L. C., 2007. Irrigation cooling effect: Regional climate forcing by land-use change. *Geophys. Res. Lett.* 34 (3), DOI: 10.1029/2006GL028679.
- Kumar, K. R., Sahai, A. K., Kumar, K. K., Patwardhan, S. K., Mishra, P. K., Revadekar, J. V., Kamala, K., Pant, G. B., 2006. High-resolution climate change scenarios for India for the 21st century. *Curr. Sci.* 90 (3), 334–345.
- Lee, E., Chase, T. N., Rajagopalan, B., Barry, R. G., Biggs, T. W., Lawrence, P. J., 2009. Effects of irrigation and vegetation activity on early Indian summer monsoon variability. *Int. J. Climatol.* 29 (4), 573–581.
- Li, C. F., Yanai, M., 1996. The onset and interannual variability of the Asian summer monsoon in relation to land sea thermal contrast. *J. Clim.* 9 (2), 358–375.
- Li, S., Perlwitz, J., Quan, X., Hoerling, M. P., 2008. Modelling the influence of North Atlantic multidecadal warmth on the Indian summer rainfall. *Geophys. Res. Lett.* 35 (5), DOI: 10.1029/2007GL032901.
- Lobell, D., Bala, G., Duffy, P., 2006. Biogeophysical impacts of cropland management changes on climate. *Geophys. Res. Lett.* 33 (6), DOI: 10.1029/2005GL025492.
- Lucas-Picher, P., Christensen, J. H., Saeed, F., Kumar, P., Asharaf, S., Ahrens, B., Wiltshire, A., Jacob, D., Hagemann, S., 2011. Can regional climate models represent the Indian monsoon? *J. Hydrol. Meteorol.* (accepted).

- Mahajan, P. N., Talwalkar, D. R., Chinthalu, G. R., Rajamani, S., 1995. Use of INSAT winds for better depiction of monsoon depression over Indian region. *Meteorol. Appl.* 2, 333–339.
- Majewski, D., Schrodin, R., 1994. Short description of the Europa-Modell (EM) and the Deutschland-Modell (DM) of the Deutscher Wetterdienst (DWD) as at October 1994. Report, Max-Planck-Inst. Meteorol., Hamburg, Germany, [Available from Deutscher Wetterdienst, Zentralamt, 63004 Offenbach am Main, Germany].
- May, W., 2003. The Indian summer monsoon and its sensitivity to the mean SSTs: Simulations with the ECHAM4 AGCM at T106 horizontal resolution. *J. Meteorol. Soc. Jpn.* 81, 57–83.
- Mirza, M. M. Q., Ahmed, Q. K., 2005. Climate change and water resources in South Asia. A. A Balkema Publishers, The Netherlands, ISBN: 0415364426.
- Mohanty, U. C., Raman, S., Rao, D. V. B., 2007. Editorial. *Nat. Hazards.* 42 (2), 253–255.
- Narkhedkar, S. G., Sinha, S. K., Kulkarni, P. L., Kulkarni, J. R., Mahajan, P. N., 1995. Use of INSAT winds for better depiction of monsoon depression over Indian region. *Meteorol. Appl.* 2, 333–339.
- O'Hare, G., 1997. The Indian Monsoon. *Geography* 82 (3), 218–230.
- Pal, J. S., Giorgi, F., Bi, X., Elguindi, N., Solmon, F., Gao, X., Rauscher, S. A., Francisco, R., Zakey, A., Winter, J., Ashfaq, M., Syed, F. S., Bell, J. L., Diffenbaugh, N. S., Karmacharya, J., Konare, A., Martinez, D., da Rocha, R. P., Sloan, L. C., Steiner, A. L., 2007. Regional climate modeling for the developing world - The ICTP RegCM3 and RegCNET. *Bull. Amr. Meteorol. Soc.* 88 (9), 1395+.
- Park, C. K., Schubert, S. D., 1997. On the nature of the 1994 East Asia summer drought. *J. Clim.* 10, 1056–1070.
- Parthasarathy, B., Kumar, K. R., Kothwale, D. R., 1992. India summer monsoon rainfall indices, 1871-1990. *Meteorol. Mag.* 121 (1441), 174–186.
- Patra, P. K., Santhanam, M. S., Potty, K. V. J., Tewari, M., Rao, P. L. S., 2000. Simulation of tropical cyclones using regional weather prediction models. *Curr. Sci.* 79 (1), 70–78.
- Peixoto, J. P., Oort, A. H., 1984. Physics of climate. *Rev. Mod. Phys.* 56 (3), 365–429.
- Pielke, R. A., 2001. Influence of the spatial distribution of vegetation and soils on the prediction of cumulus convective rainfall. *Rev. Geophys.* 39 (2), 151–177.
- Prasad, V. S., Hayashi, T., 2007. Active, weak and break spells in the Indian summer monsoon. *Hydrol. Earth Sys. Sci.* 95, 53–61.

Bibliography

- Puma, M. J., Cook, B. I., 2010. Effects of irrigation on global climate during the 20th century. *J. Geophys. Res.* 115, DOI: 10.1029/2010JD014122.
- Raman, C. R. V., Rao, Y. P., 1981. Blocking highs over Asia and monsoon droughts over India. *Nature* 289 (5795), 271–273.
- Ramaswamy, C., 1962. Breaks in the Indian summer monsoon as a phenomenon of interaction between the easterly and subtropical westerly jet streams. *Tellus* 14 (3), 337–349.
- Rechid, D., Jacob, D., 2006. Influence of monthly varying vegetation on the simulated climate in Europe. *Meteorol. Zeitschrift* 15 (1), 99–116.
- Rechid, D., Raddatz, T. J., Jacob, D., 2009. Parameterization of snow-free land surface albedo as a function of vegetation phenology based on MODIS data and applied in climate modelling. *Theo. App. Clim.* 95 (3-4), 245–255.
- Roeckner, E., Arpe, K., Bengtsson, L., Christoph, M., Claussen, M., Dumenil, L., Esch, M., Giorgetta, M., Schlese, U., Schulzweida, U., September 1996. Atmospheric general circulation model ECHAM-4: model description and simulation of present-day climate. Report 218, Max-Planck-Inst. Meteorol., Hamburg, Germany.
- Sacks, W. J., Cook, B. I., Buening, N., Levis, S., Helkowski, J. H., 2009. Effects of global irrigation on the near-surface climate. *Clim Dyn.* 33 (2-3), 159–175.
- Saeed, F., Hagemann, S., Jacob, D., 2009a. Impact of irrigation on South Asian Summer Monsoon . *Geophys. Res. Lett.* DOI: 10.1029/2009GL040625.
- Saeed, F., Hagemann, S., Jacob, D., 2011a. A framework for the evaluation of the South Asian summer monsoon in a regional climate model applied to REMO . *Int. J. Climatol.* DOI: 10.1002/joc.2285.
- Saeed, F., Hagemann, S., Jacob, D., 2011b. Influence of mid-latitude circulation on upper Indus basin precipitation: the explicit role of irrigation . *Int. J. Climatol.* (Submitted).
- Saeed, F., Jehangir, S., Noaman-ul Haq, M., Shafeeq, W. Hashmi, Z., Ali, G., Khan, A. M., 2009b. Application of UBC and DHSVM Models for Selected Catchments of Indus Basin Pakistan. Tech. Rep. GCISC-RR-11, Global Change Impact Studies Centre, ISBN: 978-969-9395-10-9.
- Saeed, S., Wolfgang, A. M., Hagemann, S., Jacob, D., 2010. Circumglobal wave train and the summer monsoon over northwestern India and Pakistan: the explicit role of the surface heat low . *Clim. Dyn.* DOI: 10.1007/s00382-010-0888-x.
- Seetaramayya, P., Parasnis, S. S., Nagar, S. G., Vernekar, K. G., 1993. Thermodynamic structure of the boundary layer in relation to monsoon depression over the Bay of Bengal—A case study. *Boundary Layer Meteorol.* 65 (3), 307–314.

- Semmler, T., Jacob, D., Schlunzen, K. H., Podzun, R., 2004. Influence of sea ice treatment in a regional climate model on boundary layer values in the Fram Strait region. *Mon. Weath. Rev.* 132 (4), 985–999.
- Shukla, J., 1987. Interannual variability of monsoons. In: Fein JS, Stephens PL (eds) *Monsoons*. Wiley, London, pp. 399–464.
- Siebert, S., Doll, P., Hoogeveen, J., Faures, J., Frenken, K., Feick, S., 2005. Development and validation of the global map of irrigation areas. *Hydrol. Earth Sys. Sci.* 9 (5), 535–547.
- Sikka, D. R., Gadgil, S., 1980. On the maximum cloud zone and the ITCZ over Indian Longitudes during the southwest monsoon. *Mon. Wea. Rev.* 108 (11), 1840–1853.
- Silvestri, G., Vera, C., Jacob, D., Pfeifer, S., Teichmann, C., 2009. A high-resolution 43-year atmospheric hindcast for South America generated with the MPI regional model. *Clim. Dyn.* 32 (5), 693–709.
- Singh, A. P., Mohanty, U. C., Sinha, P., Mandal, M., 2007. Influence of different land-surface processes on Indian summer monsoon circulation. *Nat. Hazards.* 42 (2), 423–438.
- Singh, D., Bhadram, C. V. V., Mandal, G. S., 1995. New regression model for Indian summer monsoon rainfall. *Meteorol. Atmos. Phys.* 55 (1-2), 77–86.
- Syed, F. S., Giorgi, F., Pal, J. S., King, M. P., 2006. Effect of remote forcings on the winter precipitation of central southwest Asia part 1: observations. *Theo. Appl. Climatol.* 86 (1-4), 147–160.
- Torrence, C., Webster, P. J., 1999. Interdecadal changes in the ENSO-monsoon system. *J. Clim.* 12 (8), 2679–2690.
- Uppala, S., Kallberg, P., Simmons, A., Andrae, U., Bechtold, V., Fiorino, M., Gibson, J., Haseler, J., Hernandez, A., Kelly, G., Li, X., Onogi, K., Saarinen, S., Sokka, N., Allan, R., Andersson, E., Arpe, K., Balmaseda, M., Beljaars, A., Van De Berg, L., Bidlot, J., Bormann, N., Caires, S., Chevallier, F., Dethof, A., Dragosavac, M., Fisher, M., Fuentes, M., Hagemann, S., Holm, E., Hoskins, B., Isaksen, L., Janssen, P., Jenne, R., McNally, A., Mahfouf, J., Morcrette, J., Rayner, N., Saunders, R., Simon, P., Sterl, A., Trenberth, K., Untch, A., Vasiljevic, D., Viterbo, P., Woollen, J., 2005. The ERA-40 re-analysis. *Q. J. R. Meteorol. Soc.* 131 (612), 2961–3012.
- Wang, B., Fan, Z., 1999. Choice of south Asian summer monsoon indices. *Bull. Ame. Meteorol. Soc.* 80 (4), 629–638.
- Wang, B., LinHo, 2002. Rainy season of the Asian-Pacific summer monsoon. *J. Clim.* 15 (4), 386–398.

Bibliography

- Webster, P. J., Magana, V. O., Palmer, T. N., Shukla, J., Tomas, R. A., Yanai, M., Yasunari, T., 1998. Monsoons: Processes, predictability, and the prospects for prediction. *J. Geophys. Res.-Ocn.* 103 (C7), 14451–14510.
- Webster, P. J., Yang, S., 1992. Monsoon and ENSO: Selectively Interactive Systems. *Quart. J. Royal Meteorol. Soc.* 118 (507, Part B), 877–926.
- World-Bank, 2008. World Development Report 2008, Agriculture for Development. Washington DC, doi: 10.1596/978-0-8213-7235-7.
- Yadav, R. K., 2009. Role of equatorial central Pacific and northwest of North Atlantic 2-metre surface temperatures in modulating Indian summer monsoon variability. *Clim. Dyn.* 32 (4), 549–563.
- Yadav, R. K., Yoo, J. H., Kucharski, F., Abid, M. A., 2010. Why Is ENSO Influencing Northwest India Winter Precipitation in Recent Decades? *J. Clim.* 23 (8), 1979–1993.
- Yatagi, A., , Yasunari, T., 1995. Interannual variations of summer precipitation in the arid/semi-arid regions in China and Mongolia: their regionality and relation to Asian monsoon. *J. Meteorol. Soc. Jpn.* 73, 909–923.

